



GEORG-AUGUST-UNIVERSITÄT  
GÖTTINGEN

# Master Thesis

Multivariate modelling of the dependency  
structure between article sales of a  
sportswear manufacturer

Author

**Petros Christanas**

from Nuremberg

Matriculation Number

11604278

Applied Statistics M.Sc.

Chair of Statistics and Econometrics

Supervisors

**Prof. Dr. Thomas Kneib**

**Dipl.-Vw. Quant. Fabian H. C. Raters**

Submitted July 16, 2020

Processing time of 20 weeks



## **Confidentiality Clause**



## **Statutory Declaration**



## Acknowledgments





# Contents

<b>1</b>	<b>Introduction</b>	<b>1</b>
1.1	adidas . . . . .	1
1.2	Data Sources . . . . .	3
<b>2</b>	<b>Statistical Theory &amp; Methods</b>	<b>5</b>
2.1	Shapiro-Wilk Test of Normality . . . . .	5
2.2	Generalized Linear Models . . . . .	5
2.3	Additive Models . . . . .	6
2.4	Generalized Additive Models for Location, Scale and Shape . . . . .	8
<b>3</b>	<b>Copulas &amp; Dependence Structures</b>	<b>11</b>
3.1	Introduction to Copulas . . . . .	11
3.2	Copula Classes . . . . .	14
3.2.1	Fundamental Copulas . . . . .	14
3.2.2	Elliptical Copulas . . . . .	15
3.2.3	Archimedean Copulas . . . . .	17
3.3	Dependence Measures . . . . .	20
3.3.1	Linear Correlation . . . . .	20
3.3.2	Rank Correlation . . . . .	21
3.3.3	Tail Dependence . . . . .	22
3.4	Structured Additive Conditional Copulas . . . . .	23
3.5	Vine Copulas . . . . .	24
<b>4</b>	<b>Data Exploration</b>	<b>25</b>
4.1	Universal Sales Patterns . . . . .	26
4.2	Grouped Patterns - Key Category Cluster . . . . .	31
<b>5</b>	<b>Modelling</b>	<b>35</b>
5.1	Key Category Cluster Marginals . . . . .	35
5.1.1	Key Category Cluster 2 . . . . .	35
5.1.2	Key Category Cluster 6 . . . . .	41
5.1.3	Key Category Cluster 8 . . . . .	47
5.2	KCC Correlations . . . . .	52
5.3	Article Correlations . . . . .	52

5.3.1 Data Delimitation . . . . .	53
<b>6 Conclusion</b>	<b>55</b>
<b>List of Abbreviations</b>	<b>57</b>
<b>List of Figures</b>	<b>59</b>
<b>List of Tables</b>	<b>61</b>
<b>References</b>	<b>63</b>

# 1 Introduction

Nowadays, online shopping is gradually becoming people's favourite purchasing standard. As designer and fashion brands adjust to this new way of shopping, they are not only promoting their products via third party providers, but also have their own e-Commerce websites. Likewise, *adidas* has grown its eCom channel tremendously over the past few years and has gained a large pool of casual and regular customers.

The aim of some use cases of the adidas Advanced Analytics Hub is to generate sales<sup>1</sup> forecasts for individual articles, usually on a weekly or monthly level. This is not always trivial since industrial big data are quite noisy, e.g. different types of campaigns and promotions influence the demand quantity dramatically over time. Another latent effect is sales cannibalization between newer and older articles or articles of similar traits. To identify this effect in a quantifiable way, the purpose of this thesis is to capture a dependence structure between article demand quantities over time, applied to transactional eCom data.

In the remaining of Chapter 1, a brief overview of the sports brand adidas is given in Section 1.1 and in Section 1.2 we will have a first look into our data sources and a data dictionary. Chapter 2 introduces some notions on relevant statistical methodology. In Chapter 3, we will have a closer look into the copula framework which comprises the major ingredient of the modelling part of this thesis. In Chapter 4 we perform some exploratory data analysis to deep dive into the behaviour of article sales and to step-wise investigate some hierarchical properties of our data. Chapter 5 analyses the results of modelling copulas to the data and we will examine some diagnostics using different approaches. A final conclusion will be summarized in Chapter 6, where we point out the main findings of this thesis.

## 1.1 adidas

After World War II, the "*Dassler Brothers Shoe Factory*" (German: "*Gebrüder Dassler Schuhfabrik*"), which was led by *Adolf Dassler* (aka *Adi Dassler*) and his brother Rudolph, was dissolved. The brothers split up and formed their own firms. As a result, the sports shoe factory "*Adi Dassler adidas Sportschuhfabrik*" was founded on August 18th 1949

---

<sup>1</sup>By sales we actually mean sale quantities in units throughout this thesis

by Adolf Dassler in Herzogenaurach, a small town in Germany [adidas-group.com].



(a) adidas Performance



(b) adidas Originals

Figure 1.1: Two of the adidas-group logos: Performance (left) & Originals (right)  
[adidas.com media-center]

Today, just over 70 years later, the sportswear designer and manufacturer is known as the "*adidas AG*" (short: *adidas*) and is one of the world's biggest sports and fashion brands. The global headquarters of are located in the birthplace Herzogenaurach and the company is employing over 59,000 people worldwide, with *Kasper Rørsted* leading the brand as CEO since October 1st 2016. In 2019, adidas produced over 1.1 billion sports and sports lifestyle products and is nowadays sponsoring a vast range of athletes, artists and organizations across the globe (e.g. the FIFA World Cup™).

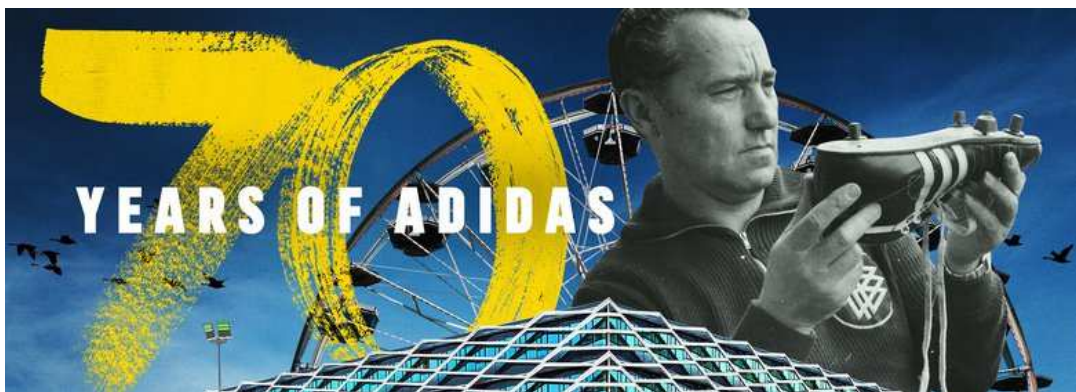


Figure 1.2: adidas celebrates its 70th anniversary and the opening of the ARENA building [adidas 70 years, 2019]

With the company's rapid growth, the data produced and acquired from social media, e-Commerce (eCom), transactions, demographics and other channels require suitable instruments and stuff to generate business relevant insights. As the need for data-driven decision making keeps increasing, "*Data and Analytics (DNA)*" became a sub-department of IT. Within DNA, the "*Data Science & AI Solutions*" team consisting of data scientists,

analysts, engineers and other roles is responsible for carrying out analytical tasks, for the most part in the context of various DNA use cases.

## 1.2 Data Sources

Throughout each season, transactional data are collected from online purchases of the sports brand's e-Commerce website. Specifically, weekly sales data for western European countries consisting of 109 observed weeks in total are provided. A short description is depicted in Table 1.1.

Column	Description	Values
week_id	Calendar week of a specific year (YYYYWW)	Factors: 201648, ..., 201852
article_number	Unique article identification number (article ID)	Factors: 10669, 10, ...
min_date_of_week	Minimum date of the respective week; always a Monday (YYYY-MM-DD)	Dates: 2016-11-28, ..., 2018-12-24
art_min_price	Minimal recorded price of the article	Non-negative (integer) value
month_id	Calendar month of a specific year (YYYYMM)	Factors: 201612, ..., 201812
season	Season of year (format: SSYY) (Spring-Summer [SS]: December - May) Fall-Winter [FW]: June - November)	Factors: SS17, FW17, SS18, FW18, SS19
bf_w	Weekly "Black Friday" promotion intensity of the article	Between 0 and 1
ff_w	Weekly "Friends & Family" promotion intensity of the article	Between 0 and 1
ot_w	Weekly article promotion intensity of "Other" type	Between 0 and 1
gross_demand_quantity	Weekly amount of added articles to shopping cart	Non-negative (integer) value
base_price_locf	Retail price of the article without any discounts	Non-negative (integer) value
total_markdown_pct	Total markdown percentage of the article	Non-negative
day_of_month	Day of the month	Integers: 1 - 31
month_of_year	Month of the year	Factors: January, ..., December
year	Year	Integers: 2016, 2017, 2018
week_of_year	Week of the year	Integers: 1 - 52

Table 1.1: Transactional raw data description from online purchases of western European countries

Due to legal regulations of the company, some columns had to undergo anonymization in order for the data to be released. To ensure data protection and confidentiality, numeric variables (with exception of time-indicating columns) were transformed. As a consequence for the analysis part, most integer values were converted to float numbers. This fact should be kept in mind by the reader, since the above table serves as a reminder and reference point for the data documentation.

Another peculiarity of this setup is to be considered, too. We will often refer to the variable *gross demand quantity* as *sales*, even though it is obviously not exactly the same. In the e-Commerce environment, there are several stages before the purchase is complete, e.g.

addition to cart, removal from cart, proceeding to checkout & even the return of bought articles. Targeting the articles added to cart, i.e. the (gross) demand quantity, provides the optimal data extraction for analytical purposes and is the closest to adequately model the dependence structure between net sales of articles.<sup>2</sup>

Besides the transactional data, attributes of the articles are provided and described in Table 1.2. Some attributes of special importance will be explained in more detail later on in Chapter 4.

Column	Description	Values (all Factors)
article_number	Unique article identification number (article ID)	10669, 10, ...
gender	Gender type of the article (Men, Women, Unisex)	M, W, U
age_group	Age group of the article (Adult, Infant, Junior, Kids)	A, I, J, K
key_category_descr	Key category of the article	KC_1, ..., KC_15
key_category_cluster_descr	Key category cluster of the article	KCC_1, ..., KCC_9
product_division_descr	Product division of the article	Apparel, Footwear, Hardware
product_group_descr	Product group of the article	Bags, Balls, Footwear Accessories, Shoes, ...
color	Consolidated color group of the article	Beige, Black, Brown, Orange, Pink, Red, ...
sports_category_descr	Sports category of the article	encoded: SC_1, ..., SC_22
sales_line_descr	Sales line of the article	encoded: SL_1, ..., SL_379
business_unit_descr	The article's Business Unit membership	encoded: BU_1, ..., BU_18
business_segment_descr	The article's Business Segment membership	encoded: BS_1, ..., BS_49
sub_brand_descr	Sub-brand of the article	encoded: sub-brand_1, ..., sub-brand_4
item_type	Item type of the article	encoded: IT_1, ..., IT_171
brand_element	Brand element of the article	encoded: BE_1, ..., BE_131
product_franchise_descr	Product franchise of the article	encoded: franchise_1, ..., franchise_72
product_line_descr	Product line of the article	encoded: PL_1, ..., PL_105
franchise_bin	Franchise indicator of the article	Franchise, Non-Franchise
category	Category of the article	encoded: category_1, category_2

Table 1.2: Article attribute data

Overall, these are the primary data sources and we will be working with data collected over two years, namely the years 2017 and 2018, while some transactions of late 2016 are attached marginally. In summary, after joining the transactional observations to the article attributes by the article ID, this translates to a dataset of over 587,000 instances and over 30 variables.

<sup>2</sup>Gross demand quantity will be our target as we follow the adidas norm

## 2 Statistical Theory & Methods

This chapter introduces some statistical methods used during the conduction of this thesis. Basic notations regarding mathematical foundations of statistics (such as linear algebra, probability theory, hypothesis testing etc) are skipped. Theoretical aspects regarding copulas and dependences structures will be introduced separately in Chapter 3.

### 2.1 Shapiro-Wilk Test of Normality

The *Shapiro-Wilk test* is a method used to test the hypothesis whether a sample of observations  $\mathbf{x} = x_1, \dots, x_n$  was drawn from a normal distribution, i.e.

$$H_0 : \mathbf{x} \sim \mathcal{N}(\mu, \sigma) \quad \text{vs} \quad H_1 : \mathbf{x} \not\sim \mathcal{N}(\mu, \sigma)$$

and the test statistic is

$$W = \frac{\left(\sum_{i=1}^n a_i x_{(i)}\right)^2}{\sum_{i=1}^n (x_i - \bar{x})^2},$$

where the coefficients  $a_i$  are given by

$$(a_1, \dots, a_n) = \frac{m^\top V^{-1}}{(m^\top V^{-1} V^{-1} m)^{1/2}}.$$

The expected values of the order statistics of independent and identically distributed (iid) random variables (RV), which are sampled from a standard normal distribution  $\mathcal{N}(0, 1)$ , are represented by the vector  $m = (m_1, \dots, m_n)^\top$  and  $V$  is the covariance matrix of those order statistics.

The Shapiro-Wilk test of normality was first introduced in Shapiro and Wilk [1965] and more details can be found in this paper.

### 2.2 Generalized Linear Models

*Generalized Linear Models (GLMs)* are an extension of the classical *Linear Regression Model (LM)*

$$y_i = \beta_0 + \beta_1 x_{i1} + \dots + \beta_k x_{ik} + \varepsilon_i, \quad i = 1, \dots, n$$

which in matrix notation can be written as

$$\mathbf{y} = \mathbf{X}\boldsymbol{\beta} + \boldsymbol{\epsilon}$$

where the response variable  $y_i$  can take values from several probability distributions (e.g. Poisson, Binomial, Gamma, ...), which are members of the exponential family [Fahrmeir

et al., 2003]. The linear predictor

$$\eta_i = \beta_0 + \beta_1 x_{i1} + \dots + \beta_k x_{ik} + \varepsilon_i = \mathbf{x}_i' \boldsymbol{\beta} \quad (2.1)$$

is passed through a *response function*  $h$  (a one-to-one, twice differentiable transformation), such that

$$E(y_i) = h(\eta_i) \quad (2.2)$$

i.e.  $h$  ensures that the expected value of the response variable belongs to the appropriate value range. The inverse of the response function, i.e.

$$g = h^{-1}, \quad (2.3)$$

is called the *link function* and transforms the mean of the response's distribution to an unbounded continuous scale.

### 2.3 Additive Models

*Additive Models* expand models with just a linear predictor

$$\eta_i^{lin} = \beta_0 + \beta_1 x_{i1} + \dots + \beta_k x_{ik}$$

(such as the LM) to

$$y_i = \eta_i^{add} + \varepsilon_i, \quad (2.4)$$

where

$$\eta_i^{add} = f_1(z_{i1}) + \dots + f_q(z_{iq}) + \eta_i^{lin}, \quad i = 1, \dots, n. \quad (2.5)$$

The functions  $f_1(z_1), \dots, f_q(z_q)$  are non-linear univariate *smooth effects* of the *continuous* covariates  $z_1, \dots, z_q$  and are defined as

$$f_j(z_j) = \sum_{l=1}^{d_j} \gamma_{jl} B_l(z_j) \quad (2.6)$$

with  $B_l(z_j)$  being *basis functions* for  $j = 1, \dots, q$  and  $d_j$  the number of basis functions for covariate  $z_j$ . The regression coefficients of the basis functions  $B_l(z_j)$  are labeled as  $\gamma_{jl}$ . There is a wide variety of basis functions which can be used to flexibly model the data in a non-parametric manner. For more content on basis functions the reader can refer to Wood [2017] and Fahrmeir et al. [2003]. The basis functions evaluated at the observed covariate values are summarized in the design matrices  $\mathbf{Z}_1, \dots, \mathbf{Z}_q$  and the additive model 2.4 can be written in matrix notation as

$$\mathbf{y} = \mathbf{Z}_1 \boldsymbol{\gamma}_1 + \dots + \mathbf{Z}_q \boldsymbol{\gamma}_q + \mathbf{X} \boldsymbol{\beta} + \boldsymbol{\varepsilon}. \quad (2.7)$$



Accordingly, the vector of function values evaluated at the observed covariate values  $z_{1j}, \dots, z_{nj}$  is denoted by  $\mathbf{f}_j = (f_j(z_{1j}), \dots, f_j(z_{nj}))'$  and therefore  $\mathbf{f}_j = \mathbf{Z}_j \boldsymbol{\gamma}_j$ . To ensure identifiability of the additive model, the smooth functions  $f_j(z_j)$  are centered around zero, such that

$$\sum_{i=1}^n f_1(z_{i1}) = \dots = \sum_{i=1}^n f_q(z_{iq}) = 0.$$

A convenient trait of additive models is that they also support the incorporation of random effects. Random coefficient terms can straightforwardly be added to the model. Data are considered to be measured in a longitudinal setting with individuals  $i = 1, \dots, m$  observed at times  $t_{i1} < \dots < t_{ij} < \dots < t_{in_i}$  or clustered data with subjects  $j = 1, \dots, n_i$  in clusters  $i = 1, \dots, m$ . Without loss of generality,<sup>3</sup> we can simply add to Equation 2.7 the terms  $\mathbf{Z}_0 \boldsymbol{\gamma}_0$  and  $\mathbf{Z}_1 \boldsymbol{\gamma}_1$  representing the design matrices and coefficients of the random intercepts and random slopes respectively. Explicitly, the coefficients are formulated as  $\boldsymbol{\gamma}_0 = (\gamma_{01}, \dots, \gamma_{0i}, \dots, \gamma_{0m})'$  and  $\boldsymbol{\gamma}_1 = (\gamma_{11}, \dots, \gamma_{1i}, \dots, \gamma_{1m})'$ , whereas the design matrices are expressed as

$$\mathbf{Z}_0 = \begin{pmatrix} \mathbf{1}_1 & & & \mathbf{0} \\ & \ddots & & \\ & & \mathbf{1}_i & \\ & & & \ddots \\ & & & & \mathbf{1}_m \end{pmatrix} \quad \mathbf{Z}_1 = \begin{pmatrix} \mathbf{x}_1 & & & \mathbf{0} \\ & \ddots & & \\ & & \mathbf{x}_i & \\ & & & \ddots \\ & & & & \mathbf{x}_m \end{pmatrix}.$$

More details and technicalities regarding mixed effects in additive models can be found in the respective literature.

Extensions of additive models to non-normal responses are consequently called *Generalized Additive Models (GAMs)*, which were first introduced by Hastie and Tibshirani [1986]. If additionally random effects are included, they are called *Generalized Additive Mixed Models (GAMMs)*.

Thus far, models with main effects and conceivably random effects have been introduced. Accordingly, these types of effects can likewise be combined with covariate interactions and/or spatial effects. Such models can be described in a unified framework and are titled as (possibly *Generalized*) *Structured Additive Regression Models (STARs)*,

$$y = f_1(\nu_1) + \dots + f_q(\nu_q) + \beta_0 + \beta_1 x_1 + \dots + \beta_k x_k + \varepsilon.$$

---

<sup>3</sup>for the indexes

The covariates  $\nu_1, \dots, \nu_q$  can be one- or multidimensional and the functions can be of different structure determining the type of effect.

## 2.4 Generalized Additive Models for Location, Scale and Shape

*Generalized Additive Models for Location, Scale & Shape (GAMLSS)* [Rigby and Stasinopoulos, 2001, 2005] are a framework which surpass the limitations that come with GLMs and GAMs. Particularly, in GAMLSS the assumption that the response variable  $y$  belongs to a distribution of the exponential family is relaxed and a more general distribution family is permissible, including highly skewed and/or kurtotic distributions. In addition, other parameters besides the mean (or location) of the response's distribution can be modelled flexibly incorporating linear, non-linear and/or additive functions of covariates as well as random effects. By modelling the scale and shape parameters also, the issue of heteroscedasticity in the response is being handled. The models are fitted using maximum (penalised) likelihood estimation. Two algorithms can be used to fit the models, namely the CG and the RS algorithms, which can be looked upon in more detail in Rigby and Stasinopoulos [2005].

Independent observations  $y_i$  for  $i = 1, 2, \dots, n$  with probability (density) function  $f(y_i | \theta^i)$ , where  $\theta^i = (\theta_{i1}, \theta_{i2}, \dots, \theta_{ip})$  are assumed. Without loss of generality,  $p$  is at most 4 and the parameters are denoted as  $(\mu_i, \sigma_i, \nu_i, \tau_i)$ , where the parameter  $\mu_i$  is the location parameter,  $\sigma_i$  is the scale parameter, and  $\nu_i$  and  $\tau_i$  are characterized as shape parameters. The model can be of course applied to distributions of any kind of parametric nature. Let  $\mathbf{y} = (y_1, y_2, \dots, y_n)^\top$  be the vector of the response variable and  $g_k(\cdot)$ ,  $k = 1, 2, 3, 4$  be known monotonic link functions. Then

$$\begin{aligned} g_1(\boldsymbol{\mu}) &= \eta_1 = \mathbf{X}_1 \boldsymbol{\beta}_1 + \sum_{j=1}^{J_1} h_{j1}(\mathbf{x}_{j1}) \\ g_2(\boldsymbol{\sigma}) &= \eta_2 = \mathbf{X}_2 \boldsymbol{\beta}_2 + \sum_{j=1}^{J_2} h_{j2}(\mathbf{x}_{j2}) \\ g_3(\boldsymbol{\nu}) &= \eta_3 = \mathbf{X}_3 \boldsymbol{\beta}_3 + \sum_{j=1}^{J_3} h_{j3}(\mathbf{x}_{j3}) \\ g_4(\boldsymbol{\tau}) &= \eta_4 = \mathbf{X}_4 \boldsymbol{\beta}_4 + \sum_{j=1}^{J_4} h_{j4}(\mathbf{x}_{j4}), \end{aligned} \tag{2.8}$$

where  $\boldsymbol{\mu}, \boldsymbol{\sigma}, \boldsymbol{\nu}, \boldsymbol{\tau}$  and  $\boldsymbol{\eta}_k$  and  $\mathbf{x}_{jk}$ , for  $j = 1, \dots, J_k$  and  $k = 1, 2, 3, 4$  are vectors of length  $n$ . The explanatory variable  $X_{jk}$  evaluated at  $x_{jk}$  is described by the additive function  $h_{jk}$ .

$X_k$  are fixed design matrices and  $\beta_k$  are the parameter vectors.<sup>4</sup>

Note that the model 2.8, also known as *semi-parametric GAMLSS* model, can be extended to allow random effect terms to be included for any parameter (more details can be found in the mentioned literature for this section).

---

<sup>4</sup>According to Stasinopoulos et al. [2007], in typical applications a constant is often adequate for each of the two shape parameters.



### 3 Copulas & Dependence Structures

Multivariate distributions consist of the marginal distributions and the dependence structure between those marginals. These components can be specified separately in a single framework with the help of copula functions. This chapter introduces the concept of modelling such dependence structures with copulas, which is the main focus of this thesis. The core elements on this subject were picked up from McNeil et al. [2015] and Ruppert and Matteson [2015].

#### 3.1 Introduction to Copulas

A  $d$ -dimensional function  $C : [0, 1]^d \rightarrow [0, 1]$  is called a *copula*, if it is a Cumulative Distribution Function (CDF) with uniform margins, i.e.

$$P(U_1 \leq u_1, \dots, U_d \leq u_d) = C(u_1, \dots, u_d)$$

where  $U_i$ ,  $i = 1, \dots, d$  are uniformly distributed Random Variables (RVs) in  $[0, 1]$ .

Since  $C$  is a CDF, following properties emerge:

- $C(\mathbf{u}) = C(u_1, \dots, u_d)$  is increasing in each component  $u_i$ ,  $i = 1, \dots, d$ .
- The  $i^{th}$  marginal distribution is obtained by setting  $u_j = 1$  for  $j \neq i$  and it has to be uniformly distributed

$$C(1, \dots, 1, u_i, 1, \dots, 1) = u_i$$

- For  $a_i \leq b_i$ , the probability  $P(U_1 \in [a_1, b_1], \dots, U_d \in [a_d, b_d])$  must be non-negative, so we obtain the *rectangle inequality*

$$\sum_{i_1=1}^2 \dots \sum_{i_d=1}^2 (-1)^{i_1 + \dots + i_d} C(u_{1,i_1}, \dots, u_{d,i_d}) \geq 0, \quad (3.1)$$

where  $u_{j,1} = a_j$  and  $u_{j,2} = b_j$ .

The reverse is also true, i.e. any function  $C$  that satisfies the above properties is a copula. Furthermore,  $C(1, u_1, \dots, u_{d-1})$  is also a  $(d-1)$ -dimensional copula and thus all  $k$ -dimensional marginals with  $2 < k < d$  are copulas.

#### Generalized Inverse

For a CDF, the *generalized inverse* is defined by

$$F^{\leftarrow}(y) := \inf\{x : F(x) \geq y\}$$

(similar to the definition of a *quantile function*).

□

### Probability Transformation

If a RV  $Y$  has a continuous CDF  $F$ , then

$$F(Y) \sim U[0, 1]. \quad (3.2)$$

□

The reverse of the *probability transformation* is the *quantile transformation*.

### Quantile Transformation

If  $U \sim U[0, 1]$  and  $F$  be a CDF, then

$$P(F^{\leftarrow}(U) \leq x) = F(x) \quad (3.3)$$

□

The above two transformations allow us to move back and forth between  $\mathbb{R}^d$  and  $[0, 1]^d$  and are the primary building blocks when it comes to copulas. Against this backdrop, *Sklar's theorem* is introduced, which is considered the foundation of all copula related applications.

### Sklar's Theorem [Sklar, 1959]

Let  $F$  be a  $d$ -dimensional CDF with marginal distributions  $F_i$ ,  $i = 1, \dots, d$ . Then there exists a copula  $C$  such that

$$F(x_1, \dots, x_d) = C(F_1(x_1), \dots, F_d(x_d)) \quad (3.4)$$

for all  $x_i \in \mathbb{R}$ ,  $i = 1, \dots, d$ .

The copula  $C$  is unique, if  $\forall i = 1, \dots, d$ ,  $F_i$  is continuous. Otherwise  $C$  is uniquely determined only on  $\text{Ran}(F_1) \times \dots \times \text{Ran}(F_d)$ , where  $\text{Ran}(F_i)$  is the range of  $F_i$ .

Conversely, if  $C$  is a  $d$ -dimensional copula and  $F_1, \dots, F_d$  are univariate CDF's, then  $F$  as defined in Equation 3.4 is a  $d$ -dimensional CDF.

□

If the copula has a Probability Density Function (PDF), then the *copula density* is defined as

$$c(\mathbf{u}) = \frac{\partial^d C(u_1, \dots, u_d)}{\partial u_1 \dots \partial u_d} \quad (3.5)$$

for a differentiable copula function  $C$  and the realization of a random vector  $\mathbf{u} = (u_1, \dots, u_d)$ .

By virtue of Equation 3.4 in Sklar's theorem and given that

$$C(\mathbf{u}) = F(F_1^{\leftarrow}(u_1), \dots, F_d^{\leftarrow}(u_d)), \quad (3.6)$$

i.e. invertible CDFs  $F_i$ ,  $i = 1, \dots, d$ , we can rewrite the copula density to

$$c(u_1, \dots, u_d) = \frac{f(F_1^{\leftarrow}(u_1), \dots, F_d^{\leftarrow}(u_d))}{\prod_{i=1}^d f_i(F_i^{\leftarrow}(u_i))} \quad (3.7)$$

for densities  $f$  of  $F$  and  $f_1, \dots, f_d$  of the corresponding marginals.

### Invariance Principal

Suppose the RVs  $X_1, \dots, X_d$  have continuous marginals and copula  $C$ . For strictly increasing functions  $T_i : \mathbb{R} \rightarrow \mathbb{R}$ ,  $i = 1, \dots, d$ , the RVs  $T_1(X_1), \dots, T_d(X_d)$  also have copula  $C$ .

□

### Fréchet-Hoeffding Bounds

Let  $C(\mathbf{u}) = C(u_1, \dots, u_d)$  be any  $d$ -dimensional copula.

Then, for

$$W(\mathbf{u}) = \max \left\{ \sum_{i=1}^d u_i - d + 1, 0 \right\} \quad (3.8)$$

as well as

$$M(\mathbf{u}) = \min_{1 \leq i \leq d} \{u_i\}, \quad (3.9)$$

it holds that

$$W(\mathbf{u}) \leq C(\mathbf{u}) \leq M(\mathbf{u}), \quad \mathbf{u} \in [0, 1]^d. \quad (3.10)$$

$W$  is called the *lower Fréchet-Hoeffding bound* and  $M$  the *upper Fréchet-Hoeffding bound*.

Note that  $W$  is a copula if and only if  $d = 2$ , whereas  $M$  is a copula for all  $d \geq 2$  (more on this later in Section 3.2.1).

□

## 3.2 Copula Classes

In this section we will take a look at three very popular *copula classes*, namely *fundamental*, *elliptical* and *archimedean copulas*. For each class, a few (parametric) *copula families*, which are widely used, will be presented.

### 3.2.1 Fundamental Copulas

Fundamental copulas are a basic class of copulas, which emerge directly from the copula framework and do not depend on any parametric components.

#### Independence Copula

It is well known that the joint CDF of a finite set of RVs  $X_i, i = 1, \dots, n$ , is equal to the product of the marginals if and only if the RVs  $X_i$  are mutually independent, i.e.

$$F_{X_1, \dots, X_n}(x_1, \dots, x_n) = \prod_{i=1}^n F_{X_i}(x_i)$$

$\forall x_1, \dots, x_n$ .

Equally, the exact same concept applies when we talk about the *independence copula*

$$\Pi(\mathbf{u}) = \prod_{i=1}^d u_i. \quad (3.11)$$

As a result of Sklar's theorem the RVs  $u_i$  are independent if and only if their copula is the independence copula, i.e.

$$C(\mathbf{u}) = \Pi(\mathbf{u})$$

and thus the copula density would be

$$c(\mathbf{u}) = 1, \quad \mathbf{u} \in [0, 1]^d.$$

□

From Equation 3.10, it is obvious that the Fréchet-Hoeffding bounds correspond to the extreme cases of perfect dependence between the RVs  $X_i, i = 1, \dots, d$ .

#### Comonotonicity Copula

Consider the RVs  $X_1, \dots, X_d$  and strictly increasing transformations  $T_1, \dots, T_d$  and  $X_i = T(X_i)$  for  $i = 2, \dots, d$ . Making use of the *invariance principle*, it can be shown that these RVs have as copula the upper Fréchet-Hoeffding bound

$$M(\mathbf{u}) = \min\{u_1, \dots, u_d\}.$$



Since there is perfect positive dependence between those RVs,  $M$  is called the *comonotonicity copula*. The number of dimensions  $d$  can be any finite number greater than or equal to 2 for  $M$  to be a copula, as the minimum remains well defined.

□

### Countermonotonicity Copula

Similar to the comonotonic case, it can be shown that if two RVs  $X_1$  and  $X_2$  are perfectly negatively dependent, their copula is the lower Fréchet-Hoeffding bound

$$W(\mathbf{u}) = \max \left\{ \sum_{i=1}^d u_i - d + 1, 0 \right\}.$$

Therefore,  $W$  is known as the *countermonotonicity copula*. Because of the fact that countermonotonicity is not valid for a dimension greater than 2, we end up with the restriction  $d = 2$  for  $W$  to be indeed a copula.

□

### 3.2.2 Elliptical Copulas

Copulas which can be derived from known multivariate distributions like for example the *Multivariate Normal (or Gaussian) Distribution* or the *Multivariate Student's t-Distribution* are called *implicit copulas*. *Elliptical copulas* are implicit copulas which arise via Sklar's theorem from elliptical distributions like the mentioned examples.

#### Gaussian Copula

Without loss of generality, for a random vector  $\mathbf{X} \sim \mathcal{N}_d(\mathbf{0}, \mathbf{P})$  and *correlation matrix*  $\mathbf{P}$ , the *Gaussian copula (family)* is given by

$$C_{\mathbf{P}}^{Ga}(\mathbf{u}) = \Phi_{\mathbf{P}} \left( \Phi^{-1}(u_1), \dots, \Phi^{-1}(u_d) \right), \quad (3.12)$$

where  $\Phi$  is the CDF of  $\mathcal{N}(0, \sigma^2)$  and  $\Phi_{\mathbf{P}}$  is the CDF of  $\mathcal{N}_d(\mathbf{0}, \mathbf{P})$ .

There are special cases to this copula family, namely for  $d = 2$  and correlation  $\rho$ , the *bivariate Gaussian copula*  $C_{\rho}^{Ga}$  is equivalent to

- the independence copula  $\Pi$  if  $\rho = 0$ ,
- the comonotonicity copula  $M$  if  $\rho = 1$  and
- the countermonotonicity copula  $W$  if  $\rho = -1$

The density of the Gaussian copula is given by

$$c_{\mathbf{P}}^{\text{Ga}}(\mathbf{u}) = \frac{1}{\sqrt{\det \mathbf{P}}} \exp \left( -\frac{1}{2} \mathbf{x}' (\mathbf{P}^{-1} - \mathbf{I}_d) \mathbf{x} \right), \quad (3.13)$$

where  $\mathbf{x} = (\Phi^{-1}(u_1), \dots, \Phi^{-1}(u_d))$ .

□

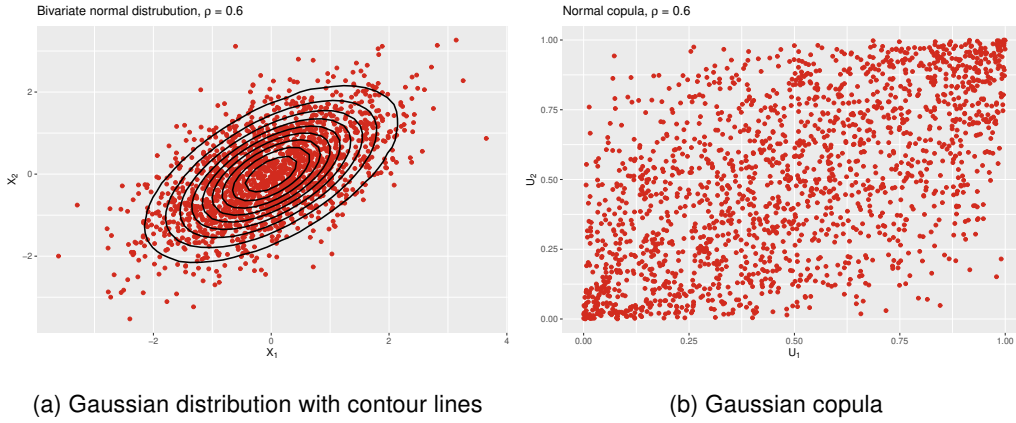


Figure 3.1: Bivariate Gaussian distribution and Gaussian copula for Pearson's  $\rho = 0.6$  and simulated sample of size  $n = 1800$ , both with standard normal marginals

### t-Copula

Consider without loss of generality  $\mathbf{X} \sim t_d(\nu, \mathbf{0}, \mathbf{P})$  (multivariate Student's t-distribution) with  $\nu$  Degrees of Freedom (d.o.f.) and  $\mathbf{P}$  a correlation matrix, then the *t-copula (family)* is given by

$$C_{\nu, \mathbf{P}}^t(\mathbf{u}) = t_{\nu, \mathbf{P}}(t_{\nu}^{-1}(u_1), \dots, t_{\nu}^{-1}(u_d)), \quad (3.14)$$

where  $t_{\nu}$  is the CDF of the univariate Student's t-distribution and  $t_{\nu, \mathbf{P}}$  is the CDF of the multivariate Student's t-distribution (both with  $\nu$  d.o.f.).

For the *bivariate t-copula* ( $d = 2$ ), the special cases are the same as for the Gaussian copula except that  $d = 0$  does not yield the independence copula (unless  $\nu \rightarrow \infty$  in which case  $C_{\nu, \rho}^t = C_{\rho}^{\text{Ga}}$ ).

The density of  $C_{\nu, \mathbf{P}}^t$  is given by

$$c_{\nu, \mathbf{P}}^t(\mathbf{u}) = \frac{\Gamma((\nu + d)/2)}{\Gamma(\nu/2)\sqrt{\det \mathbf{P}}} \left( \frac{\Gamma(\nu/2)}{\Gamma((\nu + 1)/2)} \right)^d \frac{(1 + \mathbf{x}' \mathbf{P}^{-1} \mathbf{x}/\nu)^{-(\nu + d)/2}}{\prod_{j=1}^d (1 + x_j^2/\nu)^{-(\nu + 1)/2}}, \quad (3.15)$$

where  $\mathbf{x} = (t_{\nu}^{-1}(u_1), \dots, t_{\nu}^{-1}(u_d))$ .

□

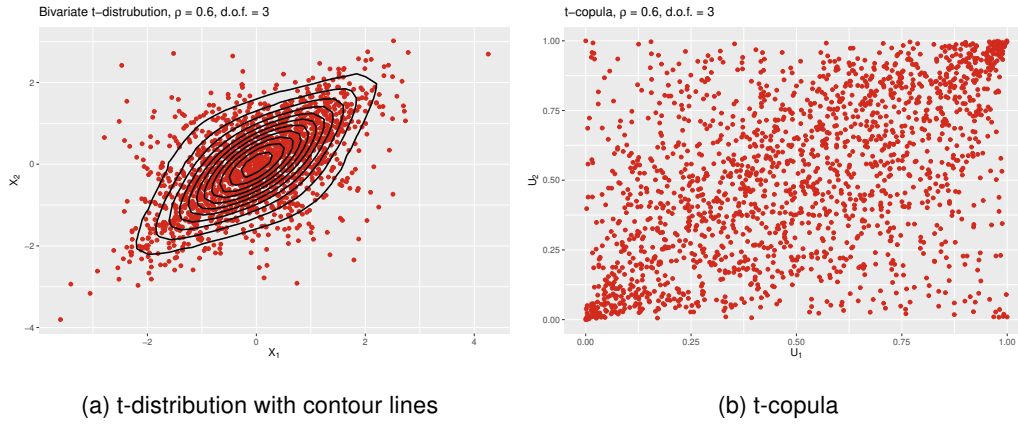


Figure 3.2: Bivariate t-distribution and t-copula with 3 degrees of freedom for Pearson's  $\rho = 0.6$  and simulated sample of size  $n = 1800$ , both with standard normal marginals

### 3.2.3 Archimedean Copulas

Unlike implicit copulas, *explicit copulas* can be specified directly by taking into account certain constructional principles. The most important aspects of a such explicit copulas, in particular *archimedean copulas*, are showcased in this subsection. Archimedean copulas are of the general form

$$C(\mathbf{u}) = \phi^{-1}(\phi(u_1) + \cdots + \phi(u_d)), \quad (3.16)$$

where the function  $\phi : [0, 1] \rightarrow [0, \infty)$  is the (*archimedean*) *generator* and satisfies the following properties:

- $\phi$  is strictly decreasing in the entire domain  $[0, 1]$
- We set  $\phi(1) = 0$
- If  $\phi(0) = \lim_{u \rightarrow 0^-} \phi(u) = \infty$ , then  $\phi$  is called *strict*.

Based on Equation 3.16 and according to the form of the generator, we can construct several copula families. Three of the most popular ones are the *Gumbel*, the *Clayton* and the *Frank copula*, which will be discussed.<sup>5</sup> The advantage of such copulas lies in the fact that they interpolate between certain fundamental dependence structures.

<sup>5</sup>We will look into these copulas for the bivariate case ( $d = 2$ ) only.

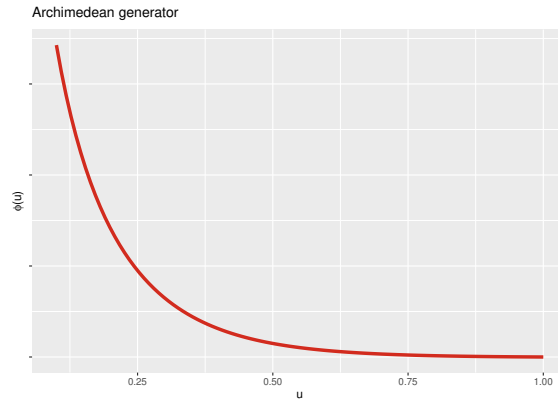


Figure 3.3: Shape of a generator function

### Clayton Copula

If the generator takes on the form

$$\phi_{Cl}(u) = \frac{1}{\theta} (u^{-\theta} - 1) \quad (3.17)$$

then we obtain the *Clayton copula* given by

$$C_{\theta}^{Cl}(u_1, u_2) = \left( \max \{ u_1^{-\theta} + u_2^{-\theta} - 1, 0 \} \right)^{-\frac{1}{\theta}}, \quad (3.18)$$

where  $\theta \in [-1, \infty) \setminus \{0\}$ .

For  $\theta > 0$  the generator of the Clayton copula is strict and we arrive at

$$C_{\theta}^{Cl}(u_1, u_2) = (u_1^{-\theta} + u_2^{-\theta} - 1)^{-\frac{1}{\theta}}. \quad (3.19)$$

Note that for  $\theta = -1$ , we obtain the lower Fréchet-Hoeffding bound  $W$ , whereas for the limits  $\theta \rightarrow 0$  and  $\theta \rightarrow \infty$  we arrive at the independence copula  $\Pi$  and the comonotonicity copula  $M$  respectively.

□

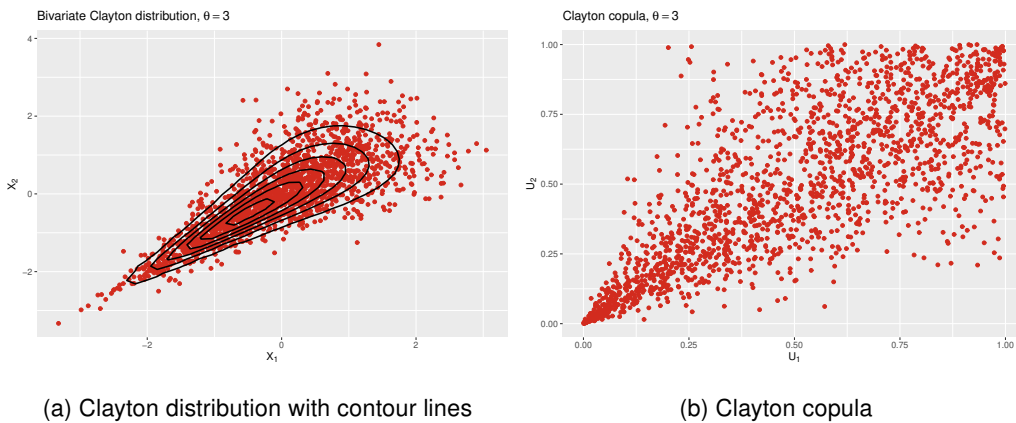


Figure 3.4: Bivariate Clayton distribution and Clayton copula for Kendall's  $\tau = 0.6$  and simulated sample of size  $n = 1800$ , both with standard normal marginals

### Gumbel Copula

If the generator takes on the form

$$\phi_{Gu}(u) = (-\ln u)^\theta, \quad \theta \in [1, \infty), \quad (3.20)$$

then we arrive at the *Gumbel copula* given by

$$C_\theta^{Gu}(u_1, u_2) = \exp \left[ - \left( (-\ln u_1)^\theta + (-\ln u_2)^\theta \right)^{\frac{1}{\theta}} \right]. \quad (3.21)$$

Note that for  $\theta = 1$ , we obtain the independence copula  $\Pi$ , while for  $\theta \rightarrow \infty$  the Gumbel copula converges to the comonotonicity copula  $M$ . Strictness holds for the entire parameter range of  $\theta$ .

□

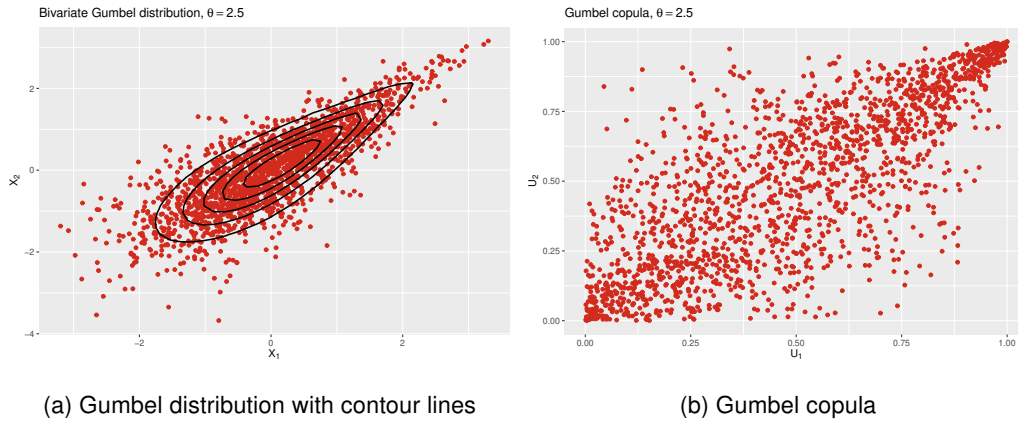


Figure 3.5: Bivariate Gumbel distribution and Gumbel copula for Kendall's  $\tau = 0.6$  and simulated sample of size  $n = 1800$ , both with standard normal marginals

### Frank Copula

If the generator takes on the form

$$-\ln \left( \frac{e^{-\theta u} - 1}{e^{-\theta} - 1} \right), \quad \theta \in \mathbb{R} \setminus \{0\}, \quad (3.22)$$

we obtain the *Frank copula* given by

$$C_\theta^{Fr}(u_1, u_2) = -\frac{1}{\theta} \ln \left( 1 + \frac{(e^{-\theta u_1} - 1) \cdot (e^{-\theta u_2} - 1)}{e^{-\theta} - 1} \right). \quad (3.23)$$

The Frank copula is strict in the parameter range of  $\theta$  and interpolates between  $W$  ( $\theta \rightarrow -\infty$ ),  $\Pi$  ( $\theta \rightarrow 0$ ) and  $M$  ( $\theta \rightarrow \infty$ ).

□

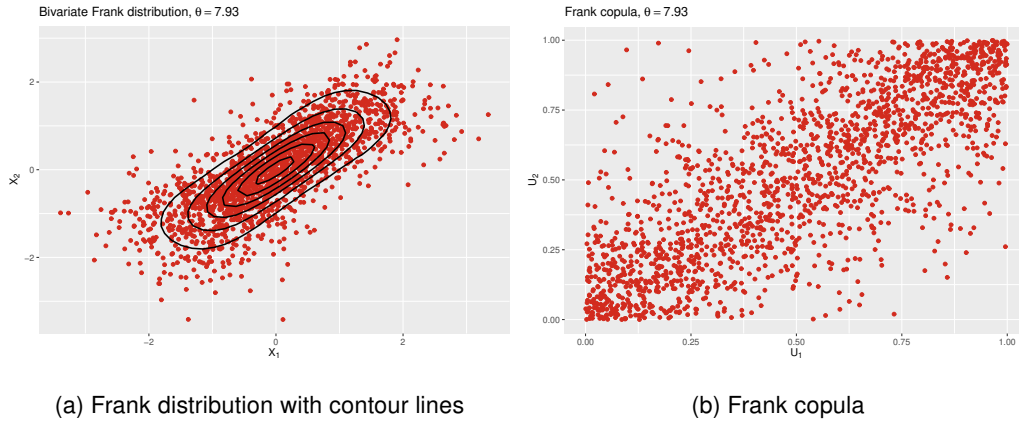


Figure 3.6: Bivariate Frank distribution and Frank copula for Kendall's  $\tau = 0.6$  and simulated sample of size  $n = 1800$ , both with standard normal marginals

### 3.3 Dependence Measures

*Dependence measures* allow us to summarize a particular kind of dependence into a single number.<sup>6</sup> Recall the Fréchet-Hoeffding bounds (Equation 3.8 and Equation 3.9). They are an example of such kind of dependence measures. After all, they represent perfect negative or positive dependence. In this section, we will take a closer look into three classes of dependence measures along with appropriate association metrics.

#### 3.3.1 Linear Correlation

Undoubtedly, the most famous association metric for two RVs  $X_1$  and  $X_2$  is the *Linear or Pearson's correlation coefficient*

$$\rho(X_1, X_2) = \frac{\text{Cov}(X_1, X_2)}{\sqrt{\text{Var}(X_1)}\sqrt{\text{Var}(X_2)}} \in [-1, 1]. \quad (3.24)$$

Note that  $E(X_1) < \infty$  and  $E(X_2) < \infty$  have to hold, i.e. the first two moments have to exist for  $\rho$  to be defined.

The Pearson correlation coefficient is interpretable for RVs which have (approximately) a linear relationship, where  $\rho = -1$  indicates perfect negative linear correlation,  $\rho = 1$  indicates perfect positive linear correlation and  $\rho = 0$  indicates no correlation between  $X_1$  and  $X_2$ . However, comprehensibility of this measure comes along with some drawbacks:

- A correlation of 0 is in general not equivalent to independence. This property holds only for normally distributed RVs.<sup>7</sup>

<sup>6</sup>In the bivariate case

<sup>7</sup>e.g.  $X_2 = X_1^2$  implies perfect dependence, yet  $\rho(X_1, X_2) = 0$ . Conversely though, independence always yields  $\rho = 0$ .

- $\rho$  is invariant only under linear transformations, but not under transformations in general.
- Given the marginals and correlation  $\rho$ , one is able to construct a joint distribution only for the class of elliptical distributions.
- Given the marginals, only for elliptically distributed RVs any  $\rho \in [-1, 1]$  is attainable.

### 3.3.2 Rank Correlation

To compensate some of the drawbacks of linear correlation, we can take advantage of correlation measures based on the ranks of data. *Rank correlation coefficients*, like the ones presented below, are always defined and obey to the invariance principal. This means that these coefficients only depend on the underlying copula and they can thereof be directly derived.

#### Spearman's Rho

Consider two RVs  $X_1$  and  $X_2$  with continuous CDFs  $F_1$  and  $F_2$ , then the *Spearman's rho correlation coefficient* is simply the linear correlation between the CDFs

$$\rho_S = \rho(F_1(X_1), F_2(X_2)). \quad (3.25)$$

The reason being is that by applying the CDF to data, naturally a multiple of the ranks of the data are obtained, which essentially is equivalent to

$$\rho_S = \rho(\text{Ran}(X_1), \text{Ran}(X_2)) \quad (3.26)$$

Due to the invariance principle, we also obtain Spearman's rho directly from the unique copula via

$$\rho_S = 12 \int_0^1 \int_0^1 C(u_1, u_2) du_1 du_2 - 3. \quad (3.27)$$

□

#### Kendall's Tau

Let  $X_1 \sim F_1$  and  $X_2 \sim F_2$  be two RV and let  $(\tilde{X}_1, \tilde{X}_2)$  be an independent copy<sup>8</sup> of  $(X_1, X_2)$ . Then *Kendall's tau* is defined by

$$\begin{aligned} \rho_\tau &= E [\text{sign}((X_1 - X'_1)(X_2 - X'_2))] \\ &= P((X_1 - X'_1)(X_2 - X'_2) > 0) - P((X_1 - X'_1)(X_2 - X'_2) < 0). \end{aligned} \quad (3.28)$$

---

<sup>8</sup>An independent copy  $\tilde{X}$  of a RV  $X$  is a RV that inherits from the same distribution as  $X$  and is independent of  $X$ .

Similarly to Spearman's rho, using the invariance principal, we can directly derive Kendall's tau from the unique copula by

$$\rho_\tau(X_1, X_2) = 4 \int_0^1 \int_0^1 C(u_1, u_2) dC(u_1, u_2) - 1. \quad (3.29)$$

□

Both  $\rho_S, \rho_\tau \in [-1, 1]$  and any value within this interval is attainable for an arbitrary copula class in contrast to the Pearson coefficient. If any of these rank correlations is  $-1$  (or  $1$ ), we are in the countermonotonic (or comonotonic) case. If  $\rho_S$  (or  $\rho_\tau$ )  $= 0$ , this does not necessarily imply independence between  $X_1$  and  $X_2$ , although the opposite direction holds. Furthermore, they are not limited to be invariant just under linear transformations.

### 3.3.3 Tail Dependence

*Coefficients of tail dependence* express the strength of the dependence in the extremes of distributions, i.e. the joint tails. We distinguish between *lower* and *upper tail dependence* between  $X_j \sim F_j, j = 1, 2$  and provided that the below limits exist, they are given by

$$\lambda_l = \lim_{q \rightarrow 0^+} P(X_2 \leq F_2^{\leftarrow}(q) | X_1 \leq F_1^{\leftarrow}(q)) \quad (3.30)$$

and

$$\lambda_u = \lim_{q \rightarrow 1^-} P(X_2 > F_2^{\leftarrow}(q) | X_1 > F_1^{\leftarrow}(q)). \quad (3.31)$$

If  $\lambda_l$  (or  $\lambda_u$ )  $= 0$ , then we say that  $X_1$  and  $X_2$  are *asymptotically independent* in the lower (or upper) tail,<sup>9</sup> otherwise we have lower (or upper) tail dependence.

For continuous CDFs and by using Bayes' theorem, these expressions can be re-written to

$$\begin{aligned} \lambda_l &= \lim_{q \rightarrow 0^+} \frac{P(X_2 \leq F_2^{\leftarrow}(q), X_1 \leq F_1^{\leftarrow}(q))}{P(X_1 \leq F_1^{\leftarrow}(q))} \\ &= \lim_{q \rightarrow 0^+} \frac{C(q, q)}{q} \end{aligned}$$

and similarly

$$\lambda_u = 2 - \lim_{q \rightarrow 1^-} \frac{1 - C(q, q)}{1 - q}.$$

Therefore, tail dependencies can be assessed by means of the copula itself when approaching the points  $(0, 0)$  and  $(1, 1)$ . In addition, for all radially symmetric copulas (e.g. the bivariate Gaussian or the t-copula) we have  $\lambda_l = \lambda_u = \lambda$ .

Some examples are:

- Clayton:  $\lambda_l = 2^{-1/\theta}, \lambda_u = 0$  (only lower tail dependence, see Figure 3.4)

<sup>9</sup>Not necessarily true for the other way around



- Gumbel:  $\lambda_l = 0$ ,  $\lambda_u = 2 - 2^{1/\theta}$  (only upper tail dependence, see Figure 3.5)
- Frank:  $\lambda_l = 0$ ,  $\lambda_u = 0$  (no tail dependence, see Figure 3.6)

Following such guidelines, the choice of a practicable copula can be facilitated. Table 3.1 displays an overview of the relationships between dependence measures and  $\theta$  parameters of various copulas.

Copula \ Measure	$\tau$	$\rho_s$	$\lambda_l$	$\lambda_u$
<b>Gaussian</b>	$\frac{2}{\pi} \arcsin(\rho)$	$\frac{6}{\pi} \arcsin(\rho)$	0	0
<b>Student's t</b>	$\frac{2}{\pi} \arcsin(\rho)$	-	$2T_{\nu+1}(\sqrt{\frac{(\nu+1)(1-\rho)}{1+\rho}})$	$2T_{\nu+1}(\sqrt{\frac{(\nu+1)(1-\rho)}{1+\rho}})$
<b>Clayton</b>	$\frac{\theta}{\theta+2}$	-	$2^{-1/\theta}$	0
<b>Gumbel</b>	$\frac{\theta-1}{\theta}$	-	0	$2 - 2^{1/\theta}$
<b>Frank</b>	$1 - \frac{4}{\theta} (4 - D_1(\theta))$	$1 - \frac{12}{\theta} (D_1(\theta) - D_2(\theta))$	0	0

Table 3.1: Bivariate relationships in copula families, with  $T_\nu$  being the Student's t-distribution function with  $\nu$  degrees of freedom and  $D_k(x) = \frac{k}{x^k} \int_0^x \frac{t^k}{e^t - 1} dt$  being the Debye function [stanfordphd]

### 3.4 Structured Additive Conditional Copulas

Modelling of the marginal response distributions along with their dependence structure has been studied so far in a strictly parametric context, not considering any potentially available covariate information. In this section, the copula framework will be broadened by adding conditions given possible covariates for all model parameters, i.e. both for the parameters of the marginals as well as the copula parameter. All involved model parameters will receive *structured additive predictors* (see Section 2.3) to account for possible non-linear or random effects. We will summarily explore *Structured Additive Conditional Copulas* and for extensive literature, good references to view are Klein and Kneib [2016], Vatter and Nagler [2019] and Marra and Radice [2016].

To get started, we define  $(Y_1, Y_2)'$  to be independent bivariate responses and  $\nu$  being the information contained in covariates. Ergo, Equation 3.4 of Sklar's theorem can be extended to the conditional case

$$F_{1,2}(Y_1, Y_2 | \nu) = C(F_1(Y_1 | \nu), F_2(Y_2 | \nu) | \nu) \quad (3.32)$$

in conjunction with all facets of Section 3.1 [Patton, 2006].

The marginal CDFs  $F_d(y_{id} | \nu_i)$  for observations  $i = 1, \dots, n$  can also be stated as

$$F_d(y_{id} | \nu_{i1}^{(d)}, \dots, \nu_{iK_d}^{(d)}), \quad d = 1, 2, \quad (3.33)$$

i.e. the distribution  $F_d$  has a total of  $K_d$  parameters, denoted as  $\vartheta_{i1}^{(d)}, \dots, \vartheta_{iK_d}^{(d)}$ . To relate all parameters of the marginals to structured additive predictors  $\eta_i^{\vartheta_k^{(d)}}$ ,  $k = 1, \dots, K_d$  consisting of the covariates  $\nu_i$  (see Section 2.3), we employ strictly increasing response mappings  $h_k^{(d)}$  to ensure proper domain allocation, i.e.

$$\vartheta_{ik}^{(d)} = h_k^{(d)}(\eta_i^{\vartheta_k^{(d)}}). \quad (3.34)$$

Assuming that the parameters of the copula can also depend on covariates  $\nu_i$  while Sklar's theorem applies as usual, the left-hand side of Equation 3.32 can equivalently be stated as

$$F_{1,2}(y_{i1}, y_{i2} | v_i) = F_{1,2}(y_{i1}, y_{i2} | \vartheta_{i1}^{(1)}, \dots, \vartheta_{iK_1}^{(1)}, \vartheta_{i1}^{(2)}, \dots, \vartheta_{iK_2}^{(2)}, \vartheta_{i1}^{(c)}, \dots, \vartheta_{iK_c}^{(c)}),$$

where the last share of parameters  $\vartheta_{i1}^{(c)}, \dots, \vartheta_{iK_c}^{(c)}$  belong to the copula. Similar to Equation 3.34, the copula parameters are modelled as  $\vartheta_{ik}^{(c)} = h_k^{(c)}(\eta_i^{\vartheta_k^{(c)}})$  with  $K_c$  being the number of parameters.

### 3.5 Vine Copulas

Vine copulas to be written down...

## 4 Data Exploration

In Section 1.2 the setup of the data to be treated was introduced. As can be seen in Table 1.2, each article can be assigned to a set of attributes. Besides some elemental attributes like *color*, *age group* or *gender*, the data exhibit a "natural" company-specific hierarchical structure. In Figure 4.1, we can see an example of such a hierarchy for the attributes *Key Category Cluster (KCC)* and *Business Segment (BS)* (See Table 1.2). The bottom level consists of the individual articles and at the top level we have the brand. It is important to mention that there are more inner levels between the brand and the articles than depicted in Figure 4.1 below. For example, Key Category (KC) would be the level below KCC. KCCs are aggregated sport/fashion categories and KCs add an additional layer to KCCs, namely the *Product Division* covering Footwear, Apparel and Accessories/Hardware. The BS supplements the KC with a consumer driven "gender" perception. Within the scope of this thesis, we will be concerned with the hierarchical structure of Figure 4.1 and in particular our KCCs of interest are "KCC 2", "KCC 6" and "KCC 8".

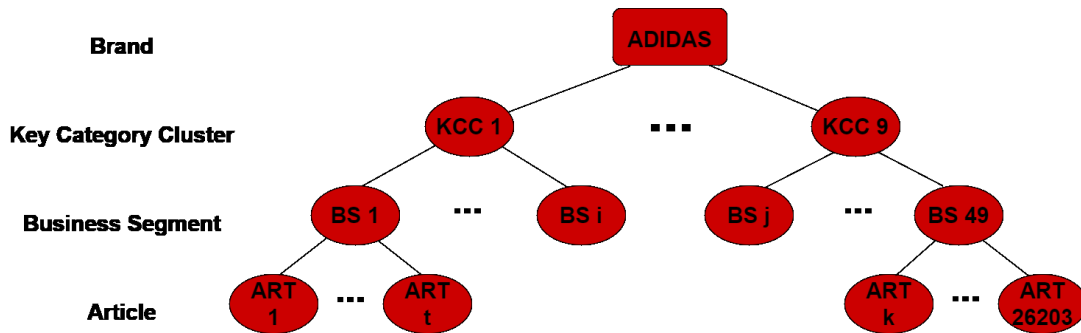


Figure 4.1: Illustration of a hierarchical article structure

Worth mentioning is that it is possible that some individual nodes might have only one single child node, meaning that the hierarchy level can stay consistent across multiple nodes. This phenomenon however is very rare and when it occurs, it affects usually two consecutive nodes only. For example, *Sub-Brand 4* has only one child node *KCC 6* (See Figure 4.2). Sub-Brands are visible for consumers through an own, not shared logo (See Figure 1.1).

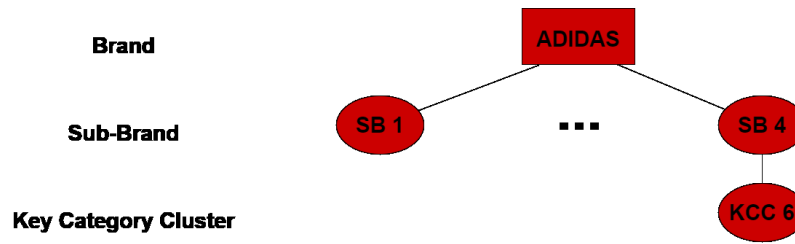


Figure 4.2: Example of a single child node

## 4.1 Universal Sales Patterns

As mentioned in Section subsection 1.2, our data contains the information about sold articles over the years 2017 and 2018. Figure 4.3 shows the weekly course for the quantities over those two years, highlighting active promotion weeks as vertical lines. We can undoubtedly recognize that "*Black Friday*" weeks (black lines) have an exceptional impact on sales, as they stand internationally for the most busy shopping periods. During these days in mid- to late November each year, large amounts of different products are heavily discounted.

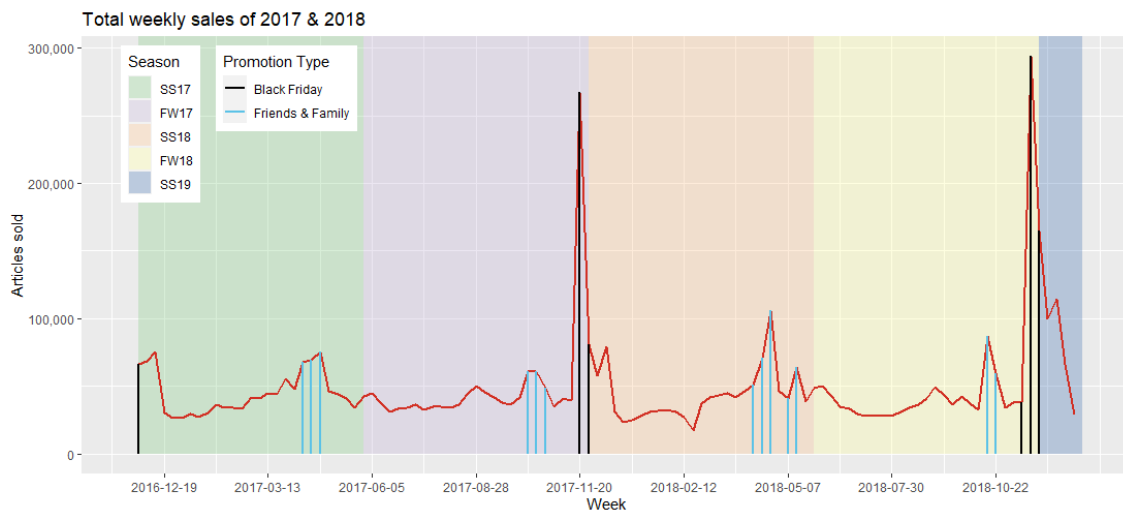


Figure 4.3: Course of article unit sales

Another promotion type we are interested in is "*Friends & Family*", occurring yearly around April-May and October, where on the eCom website plenty of articles are on offer. On these weeks, we have elevated numbers of sold articles as well (Figure 4.3, blue lines). Tables 4.1 and 4.2 show the weeks where Black Friday and Friends & Family took place respectively. The dates indicate always the Monday of the respective week (according to European standards, a week starts on Monday).

Black Friday weeks	2016-11-28	2017-11-20	2017-11-27	2018-11-12	2018-11-19	2018-11-26
--------------------	------------	------------	------------	------------	------------	------------

Table 4.1: Black Friday weeks

Friends & Family weeks	2017-04-10	2017-04-17	2017-04-24	2017-10-09	2017-10-16	2017-10-23	2018-04-09
	2018-04-16	2018-04-23	2018-05-07	2018-05-14	2018-10-15	2018-10-22	

Table 4.2: Friends & Family weeks

Figure 4.4 depicts scatterplots of 10,000 randomly chosen observations in the dataset, where the two main promotion intensities are plotted against article unit sales. A positive relationship is visible as we would expect. Due to the high noise persisting in these relationships however, Pearson’s correlation coefficient for Black Friday against sales and Friends & Family against sales take on values of 0.32 and 0.11 respectively. Similar behavioural conclusions can made about the total markdown percentage, with a correlation coefficient of 0.27 (see Figure 4.5). The type of season (Fall-Winter (FW) or Spring-Summer (SS)) doesn’t seem to make an overall difference in the sale quantities, as can be seen in Figure 4.6.

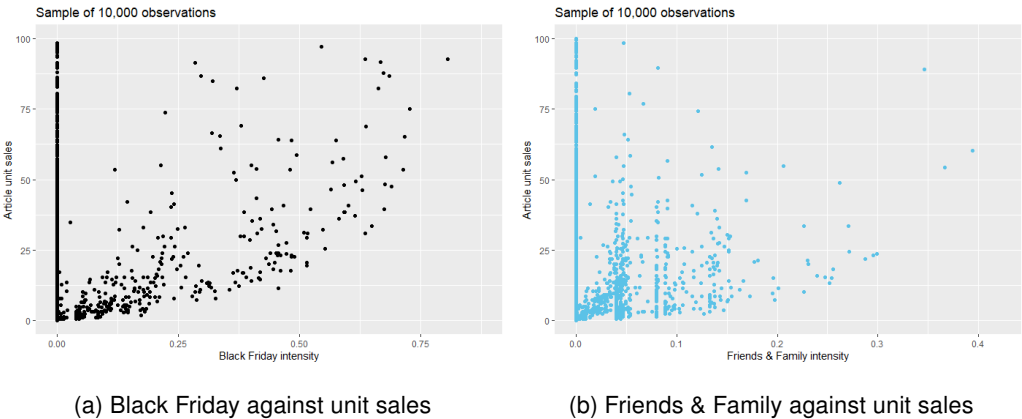


Figure 4.4: Scatterplots of promotion intensities against article unit sales; The y-axes are cut at 100

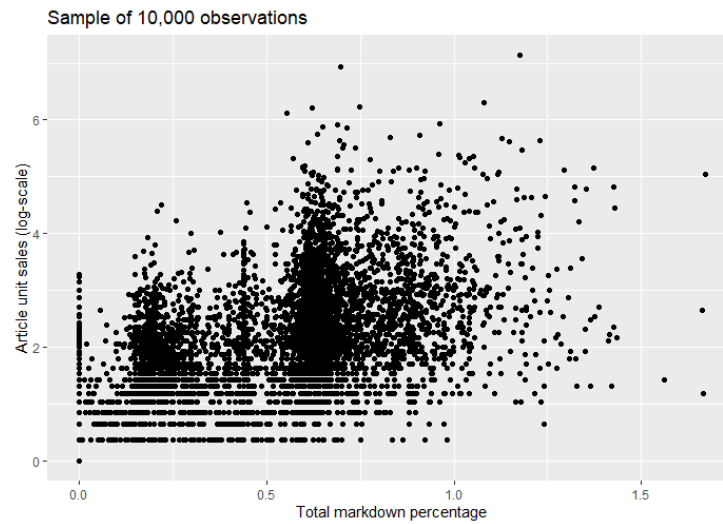


Figure 4.5: Unit sales in log-scale against total markdown percentage

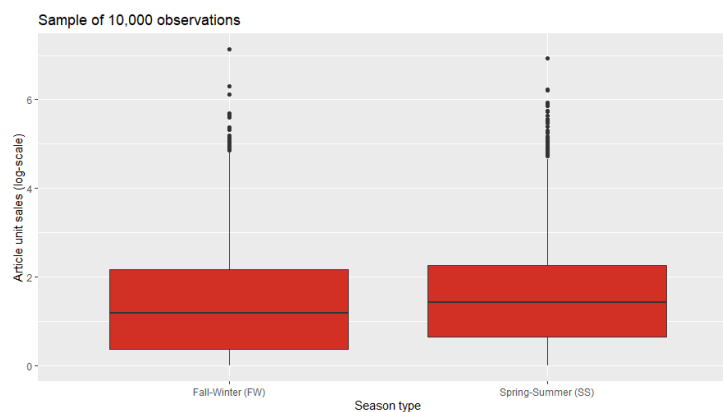
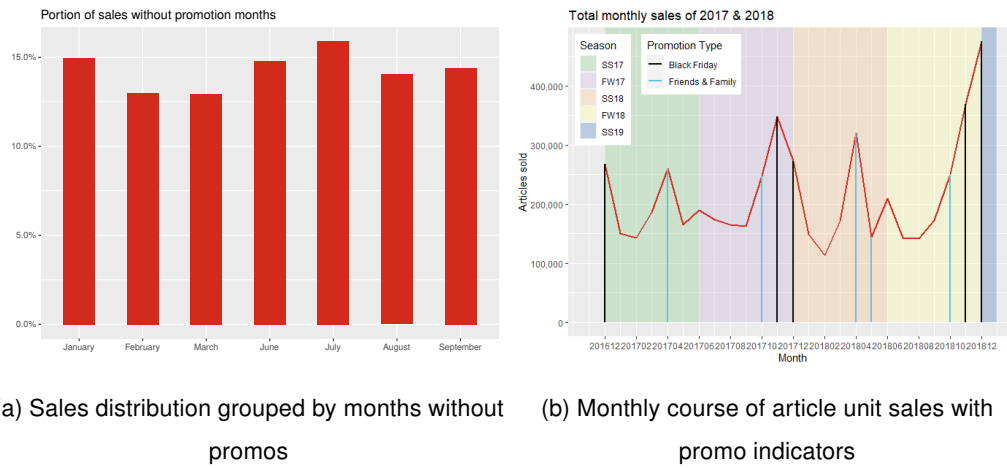


Figure 4.6: Unit sales in log-scale against season type

Regarding the months, they don't seem to differ generally in their sale quantities, that is of course excluding the months of the two mentioned promotion types. The monthly sales portions for those months can be observed in Figure 4.7a. We have slightly higher sales portions on January, June and July. Most probably this is due to Christmas and "end of the year" shopping habits, which are carried forward from December to the very next month January. Regarding June and July, they indicate summer periods and frequent occurrence of big sports events, which may drive sales. Notice that, despite the fact that December is not explicitly present in Table 4.1, it is nonetheless a Black Friday month as the promotion is still activated moving from November to December (see Figure 4.7b).



(a) Sales distribution grouped by months without promos (b) Monthly course of article unit sales with promo indicators

Figure 4.7: Monthly patterns of article unit sales

Moving forward, reviewing some sales summary statistics along with the findings so far, we detect a very high overdispersion in our data. The first two rows in Table 4.3 give as a first impression of the sales distribution. Considering the sold units of one article at a time within a week, there are lots of weeks where no single unit was sold. The median is at 2.71 units,<sup>10</sup> 75% of the "article-week" combinations take on a value of at most 20 and the minority exceeds 100 pieces (99%-quantile). The third row of the table shows how many distinct articles fall under the respective quantile of sales and there is a visible anti-proportional behaviour towards the number of sold units, which is of course intuitive. Remarkable though is the quantity of affected articles even for incredibly large quantiles.

Quantile	Min	25%	50%	75%	90%	95%	99%	99.9%	Max
# Sold units / week	0	0.45	2.71	8.14	19.45	34.39	102.71	360.12	6,816.74
# Affected articles	26,203	26,195	23,797	17,014	10,275	6,458	1,800	273	1

Table 4.3: Number of sold units per week & number of affected articles for various quantiles of sales

Conscientiously, we want to inspect the number of weekly sold units above and below a certain (large) threshold to find out how promotions influence these vast sales numbers. In Figure 4.8a we can see how the sales are distributed over Black Friday, Friends & Family and regular weeks for below a threshold of 200 units. Most high sales occurrences are not attached to any of the two big promotions. They might be due to other events or unrelated to any campaigns altogether. Observations above that threshold of 200 can be seen in Figure 4.8b and we can clearly see a change from Figure 4.8a. As expected, Black Friday is the dominating promotion type, although the majority remains

<sup>10</sup>Reminder from Section 1.2: the values are in reality discrete, but due to anonymization they were transformed into real numbers.

in not promoted sales.

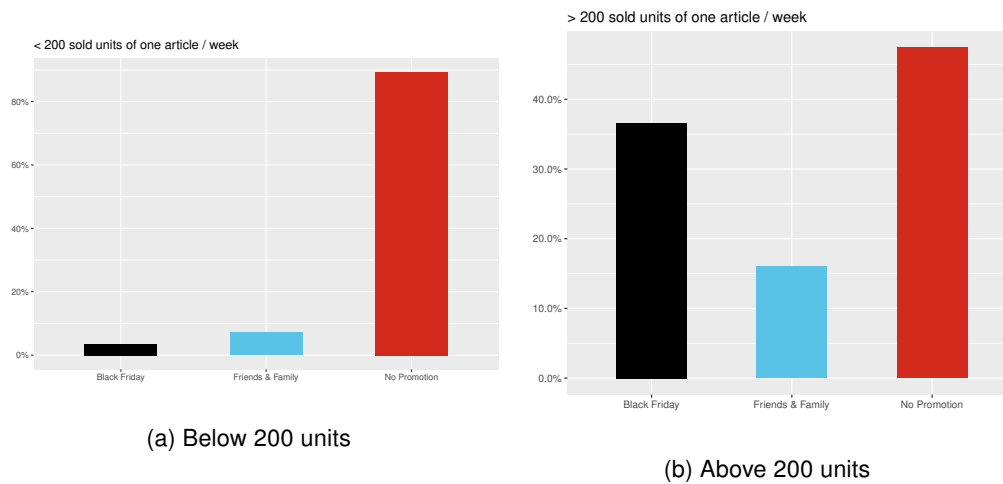


Figure 4.8: Distribution of sold units of articles per week split at 200 units

To validate the exploration on this, we may look at the empirical CDF in Figure 4.9 using all observations now. Instances with no promotions have a steeper curve (red line) and reach their maximum faster compared to articles tagged with a promotion in a certain week. The less concave curve of Friends & Family promoted sales (blue line) implies that there are more instances with a larger amount of sold units overall. The same behaviour is even more pronounced for Black Friday (black line), having considerably more high quantity instances. Along these lines, promotions might somewhat explain this pattern better.

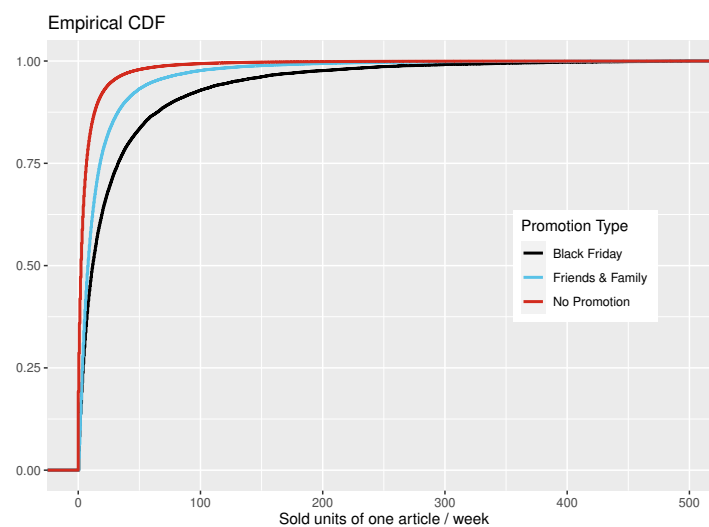


Figure 4.9: Empirical CDF of all sold units per week; x-axis cut at 500

Unfortunately, we cannot just remove such outliers with extreme sale numbers from the



dataset, as it would produce gaps in the time series of some specific articles. Removing entire articles from the analysis is also not an option at this point, since we would be forced to remove a lot of articles. There will be a data delimitation process down the line to deal with this issue (see Subsection 5.3.1). For example, 273 articles alone would have to be removed to get rid of the highest 0.01% of quantities (see Table 4.3). Besides, these extreme values might be too informative for the underlying data generating process, so we decide to keep them all.

## 4.2 Grouped Patterns - Key Category Cluster

To gain some insights on the hierarchical levels of interest, we perform some quick analysis on different groups of the upper levels of the tree in Figure 4.1. We start out with a broad picture on the key category clusters and eventually reach a better understanding for the the article behaviour.

By viewing the sales trends separately for each key category cluster, we can observe in Figure 4.10a that, among the weekly noise, they climax similarly. Just like in the previous section, those peaks come about primarily during the big promotions weeks. To put it into perspective, we can see logarithmic sales behaviour in Figure 4.10b, where patterns are quite similar although they differ strongly in volume.

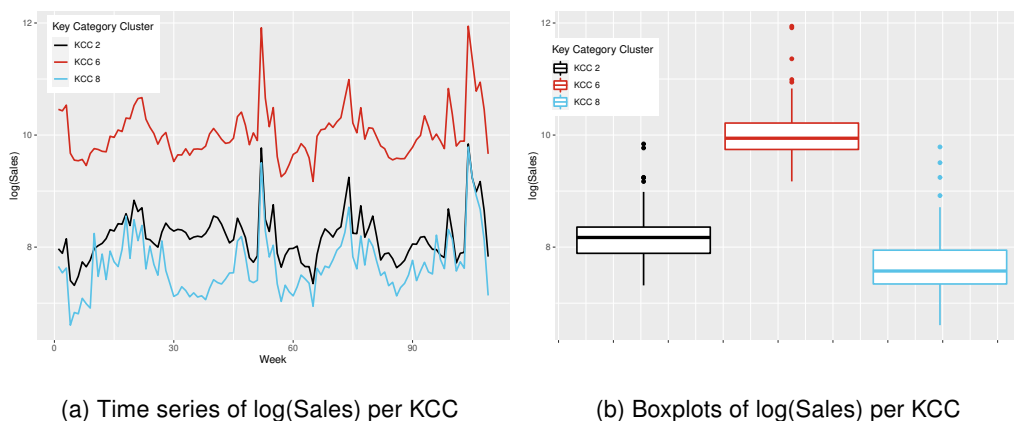


Figure 4.10: Time series and boxplot showing logarithmized sales of the key category clusters

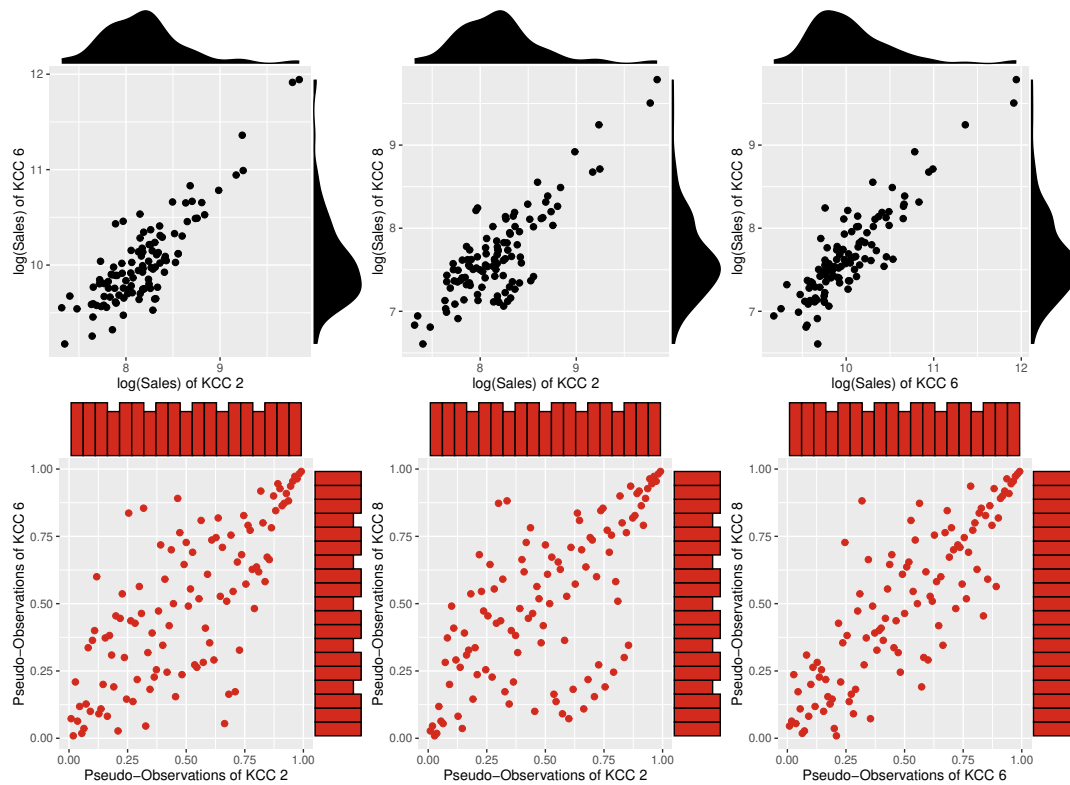


Figure 4.11: Pairwise scatterplots of sales on KCC level. First row: Logarithmic sales with marginal densities, Second row: Pseudo sales observation with marginal histograms

All the more interesting are the joint distributions of our KCCs. Figure 4.11 shows scatterplots of KCC pairs. In the first row we can see some isolated points on the upper tails representing outliers. We took the logarithmized sales to spot differences that would be otherwise hard to see. The outliers produced by the promotions still remain outliers in the log-scale. Also, by checking the densities for the marginals, pertinent marginal distributions are hardly determined but not to be ruled out.

The second row displays the pairs of the according *pseudo observations*. Pseudo observations are calculated by taking the data ranks and dividing them by  $(1 + \text{number of observations})$ , which makes them robust against outliers and restricts the value range to  $(0, 1)$ . Here we are faced with a strange behaviour of the histograms. They practically look uniformly distributed, however there are seemingly regular step patterns in the pseudo data. This might be traced back to the fact that we are dealing in reality with discrete data of not necessarily unique occurrence.

For the above reasons, on KCC level we will attempt modelling parametric distributions to the marginals as well as directly use the pseudo data. In addition, looking at both rows of Figure 4.11, we suspect tail dependence and there is an obvious strong positive corre-

lation among all three pairs, which is confirmed by viewing Figure 4.12.

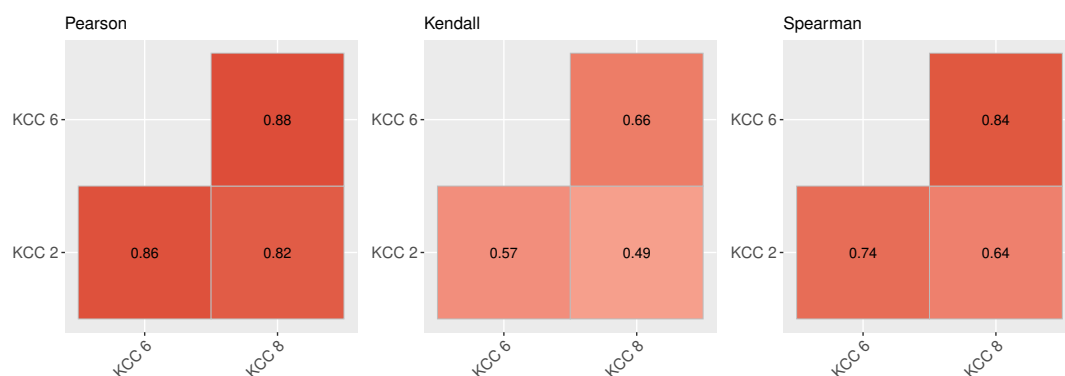


Figure 4.12: Correlation plots of the three KCC log-sales with different correlation coefficients. Left: Pearson's rho, Middle: Kendall's tau, Right: Spearman's rho

One side note on the promotion intensities of Black Friday and Friends & Family (see Table 1.1) is that on higher levels such as key category cluster, as we aggregate our data, promotion intensities become binary values indicating whether the respective promotion took place in those respective weeks. Also note that Black Friday and Friends & Family weeks do not overlap. The boxplots of the two promotion types depicted in Figure 4.13 and Figure 4.14 point out how they affect the sales. Though, one shall keep in mind that, out of 109 weeks, only the minority include promo activation. Precisely, Black Friday is activated over 6 weeks out of 109 and Friends & Family is activated over 13 weeks<sup>11</sup> (see Tables 4.1 and 4.2). In Figure 4.14, one shall also be aware of large outliers being present during no Friends & Family weeks.

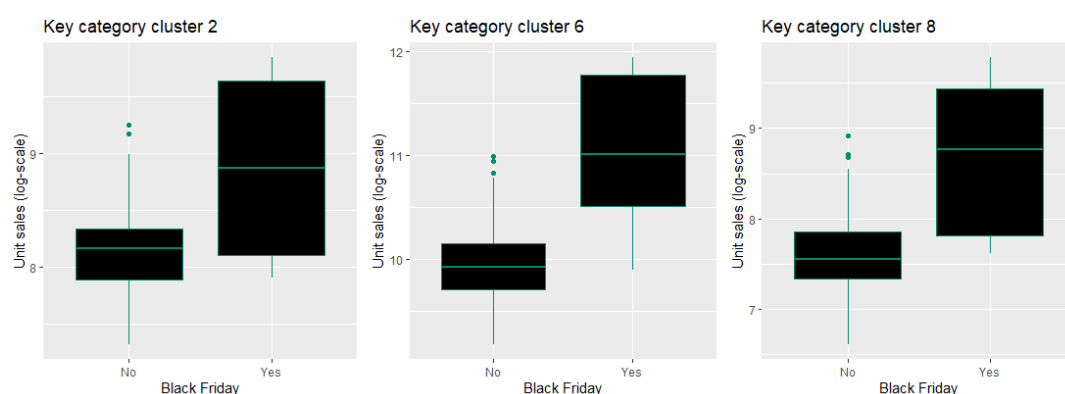


Figure 4.13: Boxplots showing log-sales of KCCs against presence of Black Friday

<sup>11</sup>And of course not in a row, as can be clearly observed in Figure 4.3.

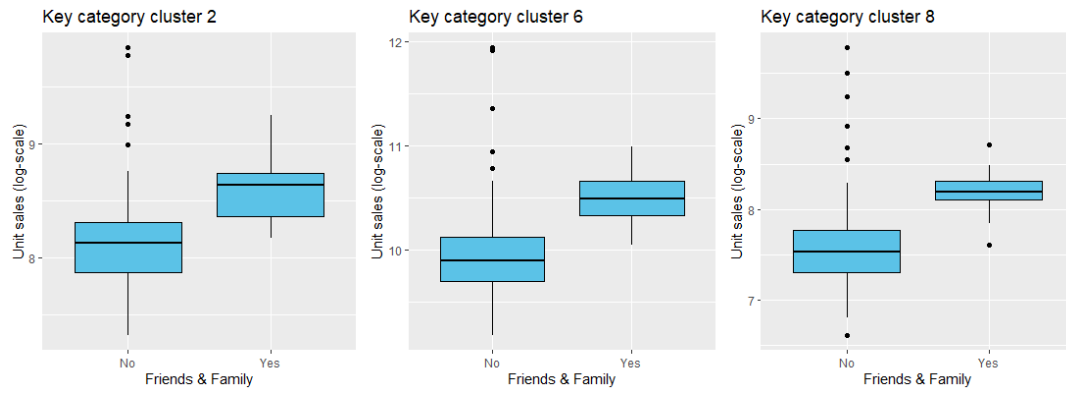


Figure 4.14: Boxplots showing log-sales of KCCs against presence of Friends & Family

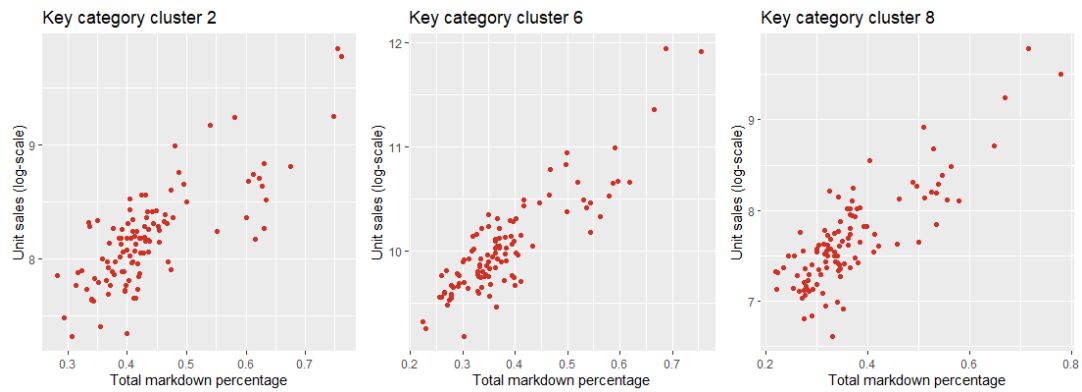


Figure 4.15: Scatterplots of KCC log-sales against total markdown percentage



Figure 4.16: Boxplots of KCC log-sales against the two season types

The scatterplots in Figure 4.15 clearly reveal the strong positive relationship between the log-sales and the KCCs' respective total markdown percentages.

Regarding the season type (SS vs FW), visual exploration is not sufficient to conclude existence of effects on the unit sales. The effect of season type as well as other features on the unit sales shall be discussed in Chapter 5.

## 5 Modelling

In this chapter, we will explore various ways on how to model, evaluate and interpret the dependence structure of unit sales.

An important aspect of the modelling part is that usually, continuous responses are implied in the literature. Nevertheless, discrete responses (like in our "real" case) are also justified when explanatory variables are involved. A detailed explanation can be found in Trivedi and Zimmer [2017].

### 5.1 Key Category Cluster Marginals

Figure 4.11 (Section 4.2) is hinting that the marginal distributions come with a noticeable skewness, which are best to take into account. The logarithmic scale is the preferred transformation due to variance stabilization of the marginals. Among a pool of possible parametric distributions, we pick an appropriate one for each marginal. Several distributions would theoretically be justifying the shape of our data, e.g. Weibull, Gamma, Box-Cox-Cole-Green or Dagum distribution. After screening those parametric distributions, we find that the exponentially modified Gaussian distribution (or exGaussian distribution which will be used from here on) fits all three marginals fairly well [Grushka, 1972].<sup>12</sup> Before entering the dependence structures between the three KCC pairs, the marginal distribution of each cluster will be analyzed individually in the next three subsections. First, the exGaussian distribution will be fitted to the marginals and in a second step covariate effects will be included to obtain flexible estimations on the distribution parameters.

#### 5.1.1 Key Category Cluster 2

Simple maximum likelihood estimation based on the log-sales of the marginals allow us to estimate the exGaussian distribution parameters. Figure 5.1a describes how the histogram of the data match to the theoretical density of an exGaussian distribution considering the estimated parameter values represented in Table 5.1.

---

<sup>12</sup>Another appropriate distribution would be the Dagum distribution [Dagum, 1975], however interpretability of the parameters is difficult to comprehend.

$\hat{\mu}$	$\hat{\sigma}$	$\hat{\nu}$
7.85	0.26	0.33

Table 5.1: Estimated parameters for log-sales of KCC 2 fitted to exGaussian distribution with no covariate effects

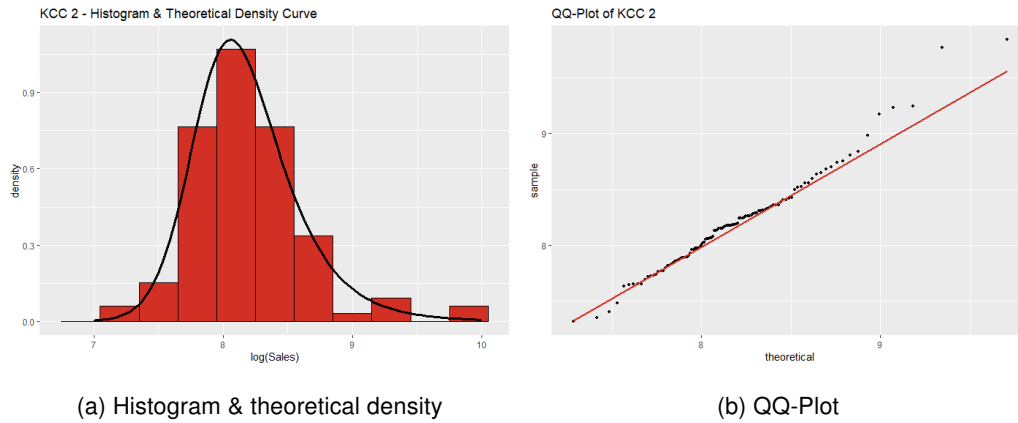


Figure 5.1: exGaussian distribution fitted to log-sales of KCC 2

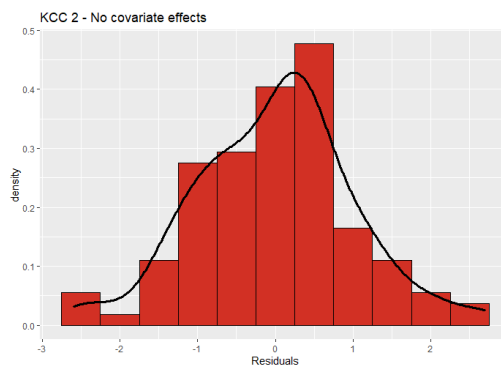


Figure 5.2: Residuals of KCC 2 log-sales fitted to an exGaussian distribution with no covariate effects together with their density curve

As can be seen in Figure 5.2, the residuals of the fitted distribution are not too far from a normal distribution. In fact, a Shapiro-Wilk normality test (see Section 2.1) will fail to reject the null hypothesis, returning a p-value of 0.6645. There still exist skewness in the distribution of the residuals and correction will be attempted in the following.

The findings so far indicate that the overall fit for this cluster is quite satisfiable and also supports interpretability of the estimated parameters.

To make the estimation more precise and to get a better understanding of what is driving sales, flexible estimation of the distribution parameters is required and thus covariate effects shall be included.

After multiple equation setups for the marginal distribution of KCC 2, the chosen GAMLSS model specification (see Section 2.4) is as follows:

$$\begin{aligned}\mu &= \beta_{01} + f_{11}(\text{time}) + f_{12}(\text{total\_markdown\_pct}) \\ \log(\sigma) &= \beta_{02} + f_{21}(\text{time}) \\ \log(\nu) &= \beta_{03},\end{aligned}\tag{5.1}$$

where the smooth functions  $f_{11}$ ,  $f_{21}$  and  $f_{12}$  are build upon P-Splines with 20 knots each. For the scale and shape parameters ( $\sigma$  and  $\nu$  respectively) the logarithmic link function is used to ensure that they are mapped to the real positive line as the exGaussian distribution family can only capture positive skewness ( $\nu$ ). For  $\sigma$  we just use time as the only regressor and we set the skewness  $\nu$  as a constant. The estimated location and scale parameters over time are depicted in Figure 5.3 and in Table 5.2 the estimated skewness parameter value with its 95% confidence interval is shown. The scale parameter has an overall increasing trend within this data spectrum and the skewness parameter is closer to zero than in the maximum likelihood approach without any covariate effects.

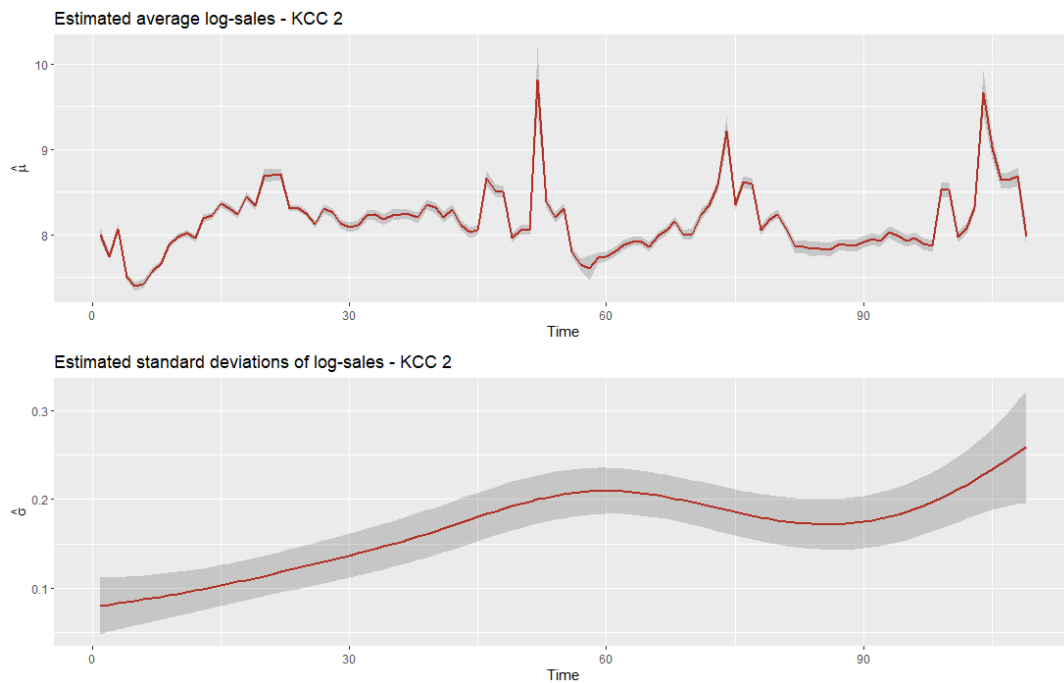


Figure 5.3: Estimated location parameter  $\hat{\mu}$  and scale parameter  $\hat{\sigma}$  with confidence bands of GAMLSS fit - KCC 2

Lower	$\hat{\nu}$	Upper
0.007	0.021	0.037

Table 5.2: Estimated skewness parameter  $\hat{\nu}$  of GAMLSS fit with 95% confidence interval bounds - KCC 2

The absence of the Black Friday and Friends & Family components in Model 5.1 is due to the fact that the effects of activated promotions to the expected sales are negative, which is contradictory to the analysis made earlier in Chapter 4.2. The output after excluding those indicator variables seem to be more stable and is also more intuitive.<sup>13</sup> Below we can observe the summary output from the R console as well as the visual covariate effects on the expected value (Figure 5.4).

```

"GAMLSS Fit on KCC 2"
*****
Family:  c("exGAUS", "ex-Gaussian")

Call:  gamlss(formula = logsales_kcc_2 ~ pb(time_obs) +
              pb(total_markdown_pct) +
              season_type,
              sigma.formula = ~pb(time_obs),
              nu.formula = ~1,
              family = "exGAUS", data = data_agg_KCC)

Fitting method: RS()

-----
Mu link function:  identity
Mu Coefficients:
              Estimate Std. Error t value Pr(>|t|)
(Intercept)    6.9696037  0.0805163  86.561  <2e-16 ***
pb(time_obs)    0.0003707  0.0005345   0.693   0.490
pb(total_markdown_pct) 3.1718822  0.1672266  18.968  <2e-16 ***
season_typeSS   -0.0254578  0.0368162  -0.691   0.491
---

```

<sup>13</sup>This might be traced back to the fact that promos obviously yield higher markdowns and thus we reach redundancy of variables in the model.



```

Signif. codes:  0 '***' 0.001 '**' 0.01 '*' 0.05 '.' 0.1 ' ' 1

-----

Sigma link function:  log
Sigma Coefficients:
              Estimate Std. Error t value Pr(>|t|)
(Intercept) -0.818893   0.160071  -5.116 1.82e-06 ***
pb(time_obs) -0.005161   0.002356  -2.191  0.0311 *
---
Signif. codes:  0 '***' 0.001 '**' 0.01 '*' 0.05 '.' 0.1 ' ' 1

-----

Nu link function:  log
Nu Coefficients:
              Estimate Std. Error t value Pr(>|t|)
(Intercept)  -3.830      1.854  -2.066  0.0418 *
---
Signif. codes:  0 '***' 0.001 '**' 0.01 '*' 0.05 '.' 0.1 ' ' 1

-----

NOTE: Additive smoothing terms exist in the formulas:
  i) Std. Error for smoothers are for the linear effect only.
 ii) Std. Error for the linear terms maybe are not accurate.

-----

No. of observations in the fit:  109
Degrees of Freedom for the fit:  21.33435
      Residual Deg. of Freedom:  87.66565
              at cycle:  20

Global Deviance:      -87.60685
              AIC:      -44.93816
              SBC:      12.48

*****
c@FancyVerbLinee*****

```

From the visual representation of the covariate effects in (Figure 5.4, we can see that until

about August of 2017 (just below the 40th time observation) the log-sales are increasing and then from November on (roughly 50th observation) the log-sales remain at a constant level with somewhat higher values end of May (just below 80th observation). The overall course of the temporal effect on the response resembles a flat wavy line around zero, which is quite aligned with the coefficient in the R-output. Higher total markdown percentages enhance higher response values, which can also be observed when looking at the R-output. The estimated coefficient for the markdown obtains a value of 3.17. The seasonal effect of Spring-Summer is slightly lower than the effect of Fall-Winter.

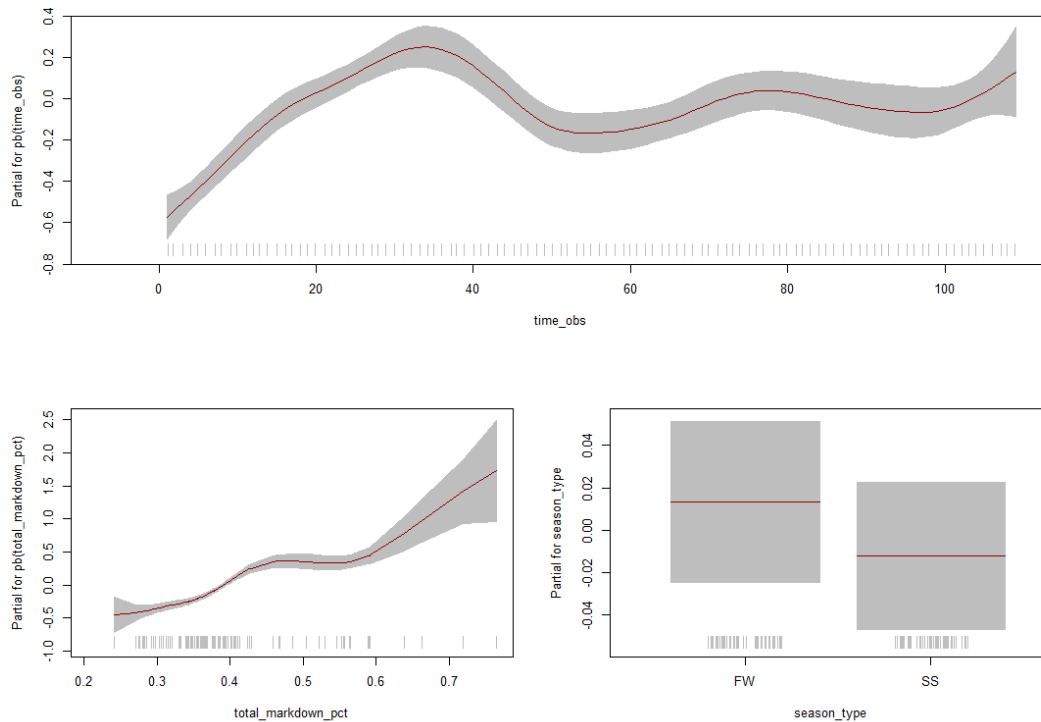


Figure 5.4: Covariate effects on the expected response variable (log-sales) of GAMLSS fit - KCC 2

Fitting the data to a GAMLSS model like this can be considered favourable. The emerged residuals are closer to a standard normal distribution than the maximum likelihood estimation without any covariate effects. Diagnostic plots of quantile residuals in Figure 5.5 confirm this. The R-output below Figure 5.5 returns a detailed summary of the estimated location, scale and shape parameters of the residuals' distribution.

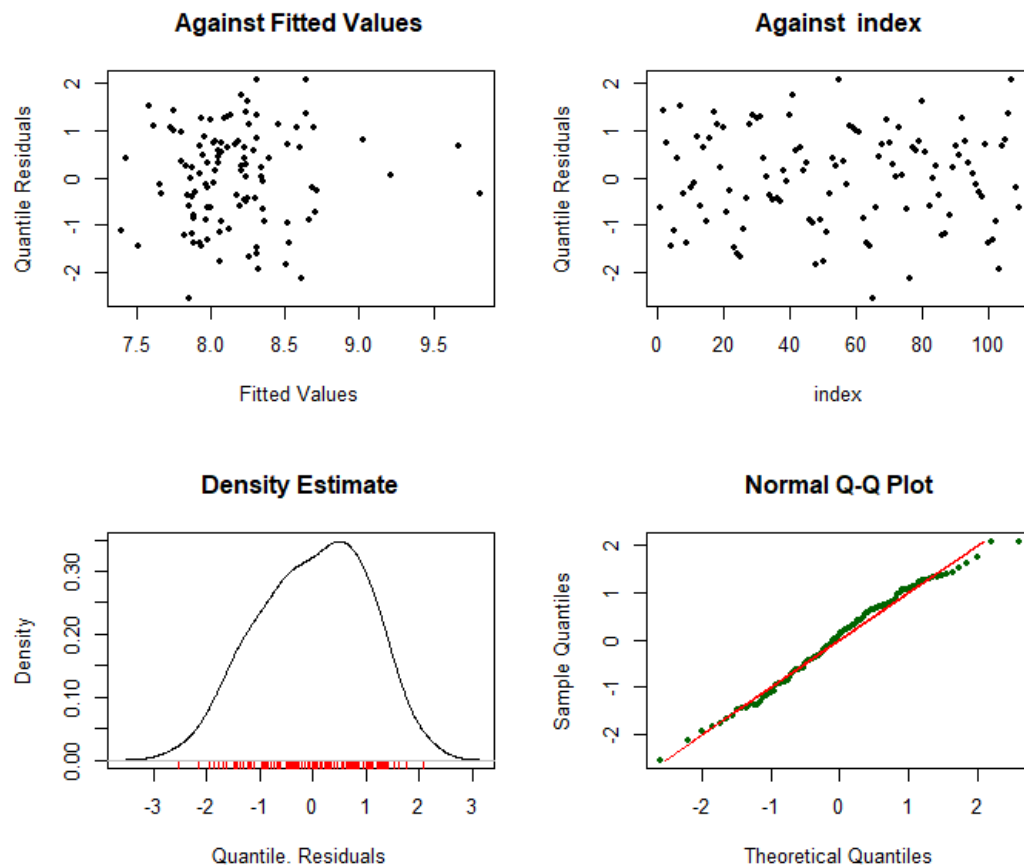


Figure 5.5: Residuals of GAMLSS fit - KCC 2

"Residuals of GAMLSS Fit on KCC 2"

```
*****
Summary of the Quantile Residuals
      mean   = 0.007148488
      variance = 1.010987
      coef. of skewness = -0.216058
      coef. of kurtosis = 2.323837
Filliben correlation coefficient = 0.9938627
*****
```

### 5.1.2 Key Category Cluster 6

The same procedure as in Subsection 5.1.2 for key category cluster 2 will be applied here to analyze the marginal distribution of the log-sales in key category cluster 6.

Excluding all covariates, simple maximum likelihood estimation results can be summarized within Table 5.3, Figure 5.6 and Figure 5.7. A Shapiro-Wilk test on the residuals

returns a p-value of 0.87 and the fails to reject the null hypothesis of non-normality.

$\hat{\mu}$	$\hat{\sigma}$	$\hat{\nu}$
9.62	0.20	0.41

Table 5.3: Estimated parameters for log-sales of KCC 6 fitted to exGaussian distribution with no covariate effects

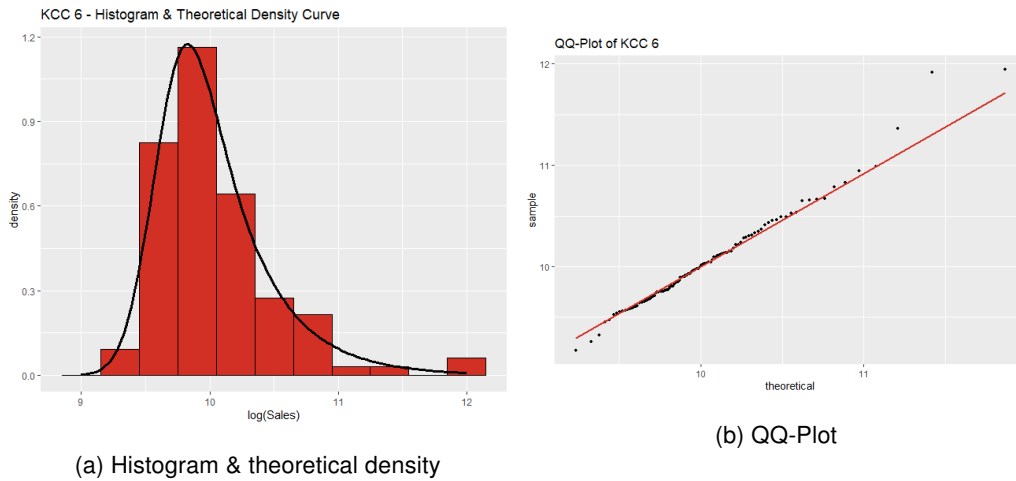


Figure 5.6: exGaussian distribution fitted to log-sales of KCC 6

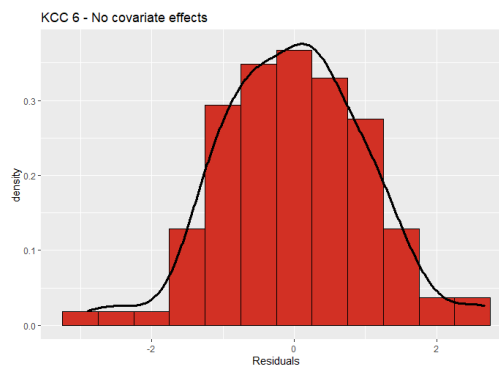


Figure 5.7: Residuals of KCC 6 log-sales fitted to an exGaussian distribution with no covariate effects together with their density curve

Reviewing different model specifications, the same issues as for KCC 2 arise when including Black Friday and Friends & Family promo activations. Therefore, the same models as in the previous Subsection is chosen (Model 5.1, exGaussian distribution family for the response variable). The estimated time-varying location and scale parameters can be seen in Figure 5.8 and the skewness parameter  $\hat{\nu}$  with 95% CI in Table 5.4. The standard deviation remains almost constant at 0.2, uncertainty taken into consideration.

```

                                "GAMLSS Fit on KCC 6"
*****
Family:  c("exGAUS", "ex-Gaussian")

Call:  gamlss(formula = logsales_kcc_6 ~ pb(time_obs) +
              pb(total_markdown_pct) +
              season_type,
              sigma.formula = ~pb(time_obs),
              nu.formula = ~1,
              family = "exGAUS", data = data_agg_KCC)

Fitting method: RS()

-----
Mu link function:  identity
Mu Coefficients:
              Estimate Std. Error t value Pr(>|t|)
(Intercept)    8.6918240   0.1010279   86.034  < 2e-16 ***
pb(time_obs)     0.0022095   0.0006587    3.355  0.00112 **
pb(total_markdown_pct) 2.9945916   0.2097409   14.278  < 2e-16 ***
season_typeSS   -0.0093005   0.0411427   -0.226  0.82161
---
Signif. codes:  0 '***' 0.001 '**' 0.01 '*' 0.05 '.' 0.1 ' ' 1

-----
Sigma link function:  log
Sigma Coefficients:
              Estimate Std. Error t value Pr(>|t|)
(Intercept)  -1.695695   0.167446  -10.13  <2e-16 ***
pb(time_obs) -0.000188   0.002354   -0.08   0.937
---
Signif. codes:  0 '***' 0.001 '**' 0.01 '*' 0.05 '.' 0.1 ' ' 1

-----
Nu link function:  log

```

Nu Coefficients:

	Estimate	Std. Error	t value	Pr(> t )
(Intercept)	-3.214	1.656	-1.94	0.0551 .

---

Signif. codes: 0 '\*\*\*' 0.001 '\*\*' 0.01 '\*' 0.05 '.' 0.1 ' ' 1

-----

NOTE: Additive smoothing terms exist in the formulas:

- i) Std. Error for smoothers are for the linear effect only.
- ii) Std. Error for the linear terms maybe are not accurate.

-----

No. of observations in the fit: 109

Degrees of Freedom for the fit: 7.010025

Residual Deg. of Freedom: 101.99

at cycle: 20

Global Deviance: -41.81131

AIC: -27.79126

SBC: -8.92484

\*\*\*\*\*

c@FancyVerbLinee\*\*\*\*\*

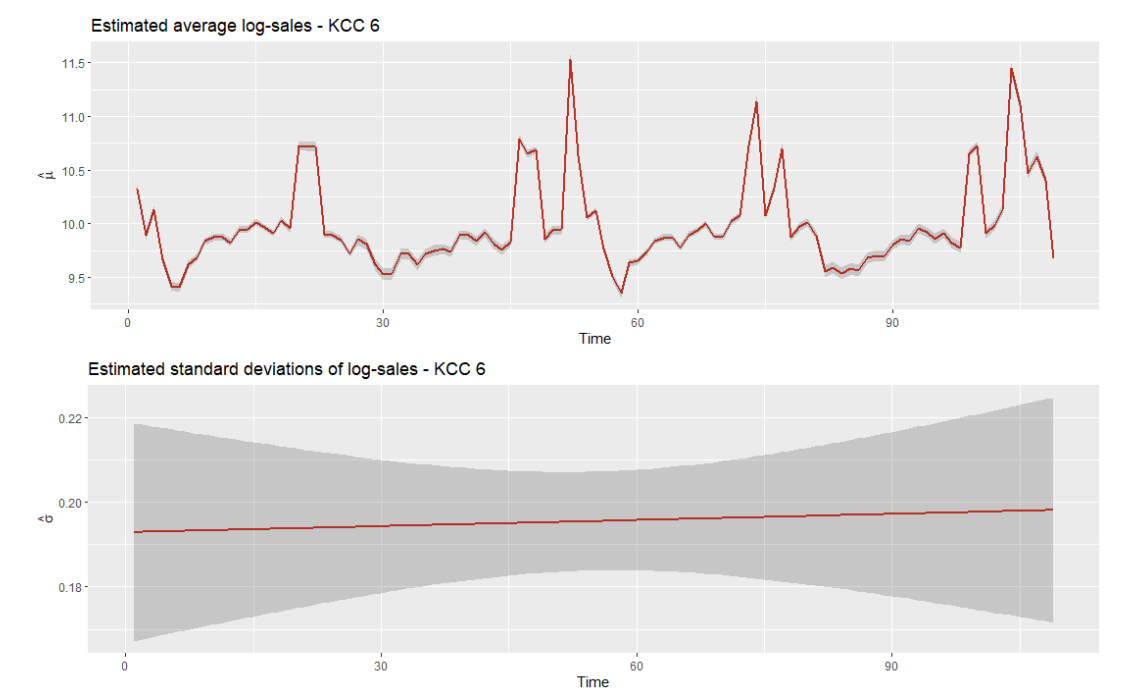


Figure 5.8: Estimated location parameter  $\hat{\mu}$  and scale parameter  $\hat{\sigma}$  with confidence bands of GAMLSS fit - KCC 6

Lower	$\hat{\nu}$	Upper
0.040	0.021	0.060

Table 5.4: Estimated skewness parameter  $\hat{\nu}$  of GAMLSS fit with 95% confidence interval bounds - KCC 6

Figure 5.9 reveals some interesting points regarding covariate effects. The temporal effect, just like the total markdown percentage, collapses to an increasing straight line. The temporal effect also exhibits symmetrical behaviour around zero, including uncertainty. Just like in KCC 2, the effect of Spring-Summer is slightly smaller than that of Fall-Winter.

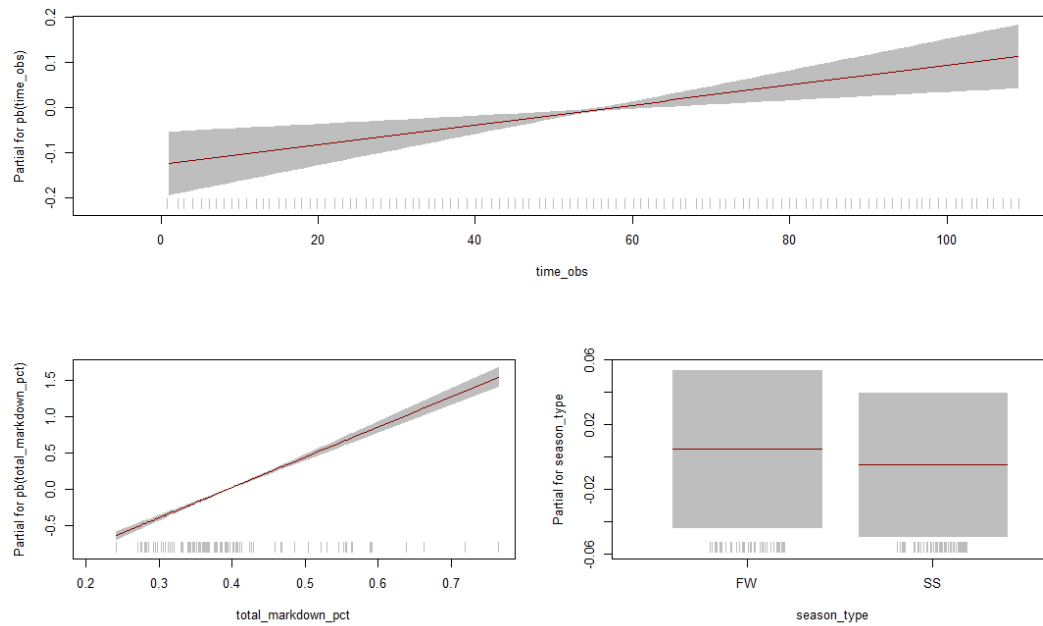


Figure 5.9: Covariate effects on the expected response variable (log-sales) of GAMLSS fit - KCC 6

Inspecting the diagnostic plots for the residuals in Figure 5.10 along with the associated summary output, we can again confirm an appropriate fit.



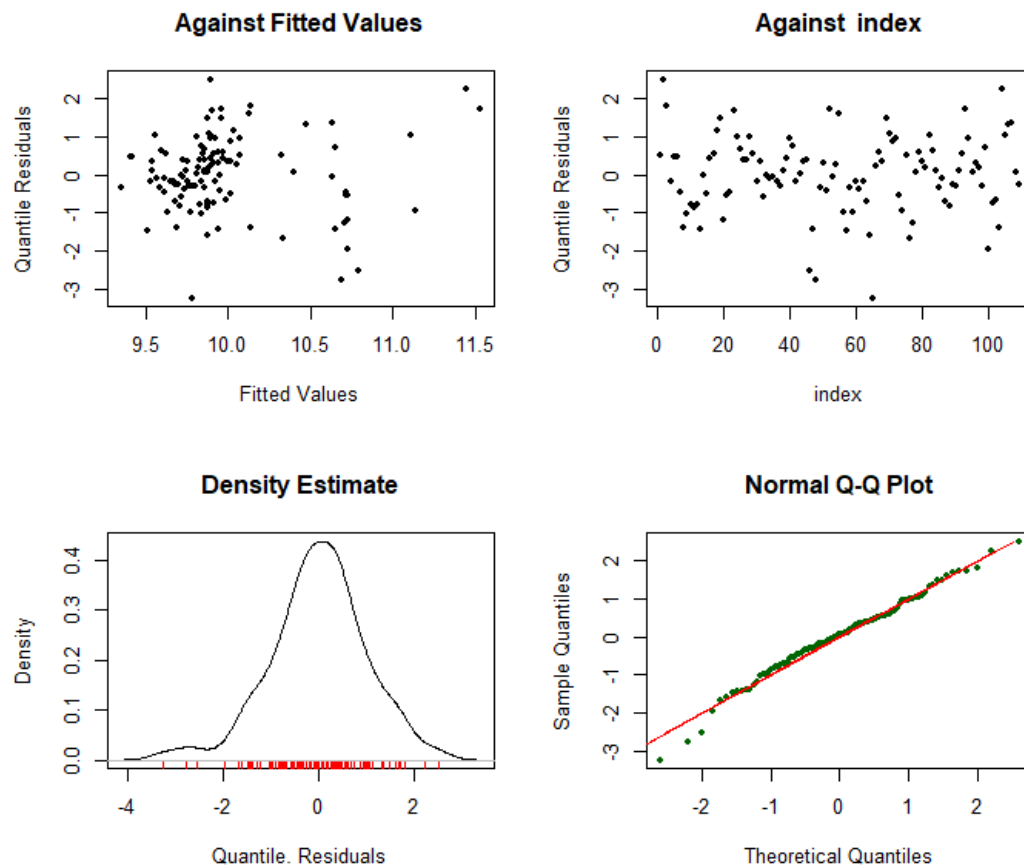


Figure 5.10: Residuals of GAMLSS fit - KCC 6

"Residuals of GAMLSS Fit on KCC 6"

```
*****
Summary of the Quantile Residuals
      mean   = 0.008536513
  variance   = 1.011009
coef. of skewness = -0.3568275
coef. of kurtosis  = 3.698673
Filliben correlation coefficient = 0.9919273
*****
```

### 5.1.3 Key Category Cluster 8

The procedure is continued also for key category cluster 8 with the same conditions, since we have similar issues as in the previous two clusters.

Table 5.5, Figure 5.11 and Figure 5.12 summarize the findings when the log-sales of KCC 8 are fitted to an exGaussian distribution with no regressors. Normality of the residuals can be assumed, as the Shapiro-Wilk test returns a p-value of 0.99 and thus fails to reject

the null hypothesis of non-normality.

$\hat{\mu}$	$\hat{\sigma}$	$\hat{\nu}$
7.21	0.27	0.46

Table 5.5: Estimated parameters for log-sales of KCC 8 fitted to exGaussian distribution with no covariate effects

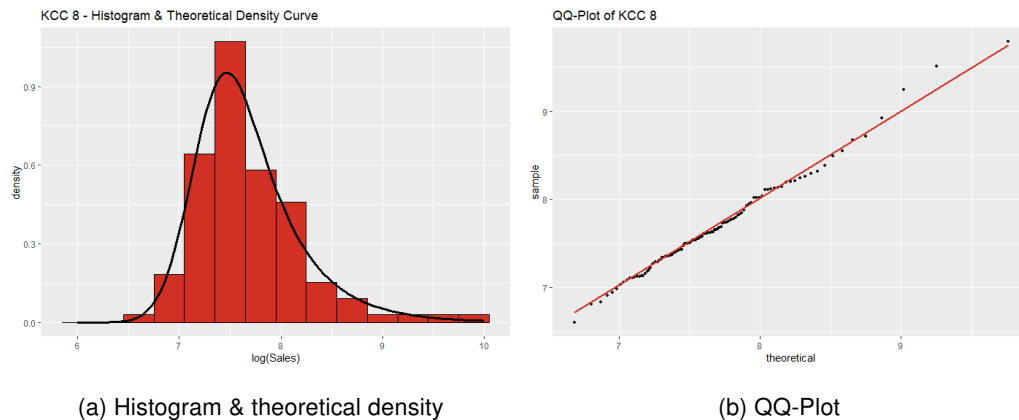


Figure 5.11: exGaussian distribution fitted to log-sales of KCC 8

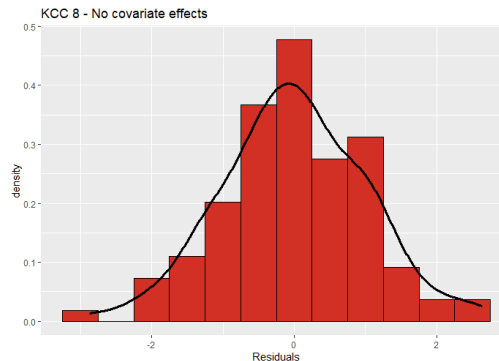


Figure 5.12: Residuals of KCC 8 log-sales fitted to an exGaussian distribution with no covariate effects together with their density curve

Again, Model 5.1 is applied to the log-sales. The summary output and estimated parameters with confidence intervals can be seen in Figure 5.13 and in Table 5.6. We notice that the variance is decreasing until November (roughly 50th observation point) and the increases again and that a low skewness remains in the data.

#### "GAMLSS Fit on KCC 8"

```
*****
Family:  c("exGAUS", "ex-Gaussian")
```

```
Call:  gamlss(formula = logsales_kcc_8 ~ pb(time_obs) +
              pb(total_markdown_pct) +
              season_type,
sigma.formula = ~pb(time_obs),
nu.formula = ~1,
family = "exGAUS", data = data_agg_KCC)
```

```
Fitting method: RS()
```

```
-----
Mu link function:  identity
```

```
Mu Coefficients:
```

	Estimate	Std. Error	t value	Pr(> t )
(Intercept)	6.0688342	0.1080385	56.173	< 2e-16 ***
pb(time_obs)	0.0052143	0.0008299	6.283	9.42e-09 ***
pb(total_markdown_pct)	2.7996474	0.2102418	13.316	< 2e-16 ***
season_typeSS	0.0307267	0.0438628	0.701	0.485

```
---
```

```
Signif. codes:  0 '***' 0.001 '**' 0.01 '*' 0.05 '.' 0.1 ' ' 1
```

```
-----
Sigma link function:  log
```

```
Sigma Coefficients:
```

	Estimate	Std. Error	t value	Pr(> t )
(Intercept)	-1.266396	0.277706	-4.56	1.49e-05 ***
pb(time_obs)	-0.005311	0.003427	-1.55	0.124

```
---
```

```
Signif. codes:  0 '***' 0.001 '**' 0.01 '*' 0.05 '.' 0.1 ' ' 1
```

```
-----
Nu link function:  log
```

```
Nu Coefficients:
```

	Estimate	Std. Error	t value	Pr(> t )
(Intercept)	-1.9415	0.3787	-5.127	1.5e-06 ***

```
---
```

Signif. codes: 0 '\*\*\*' 0.001 '\*\*' 0.01 '\*' 0.05 '.' 0.1 ' ' 1

-----  
NOTE: Additive smoothing terms exist in the formulas:

- i) Std. Error for smoothers are for the linear effect only.
  - ii) Std. Error for the linear terms maybe are not accurate.
- 

No. of observations in the fit: 109

Degrees of Freedom for the fit: 11.91903

Residual Deg. of Freedom: 97.08097

at cycle: 20

Global Deviance: -5.489673

AIC: 18.3484

SBC: 50.42666

\*\*\*\*\*

c@FancyVerbLinee\*\*\*\*\*

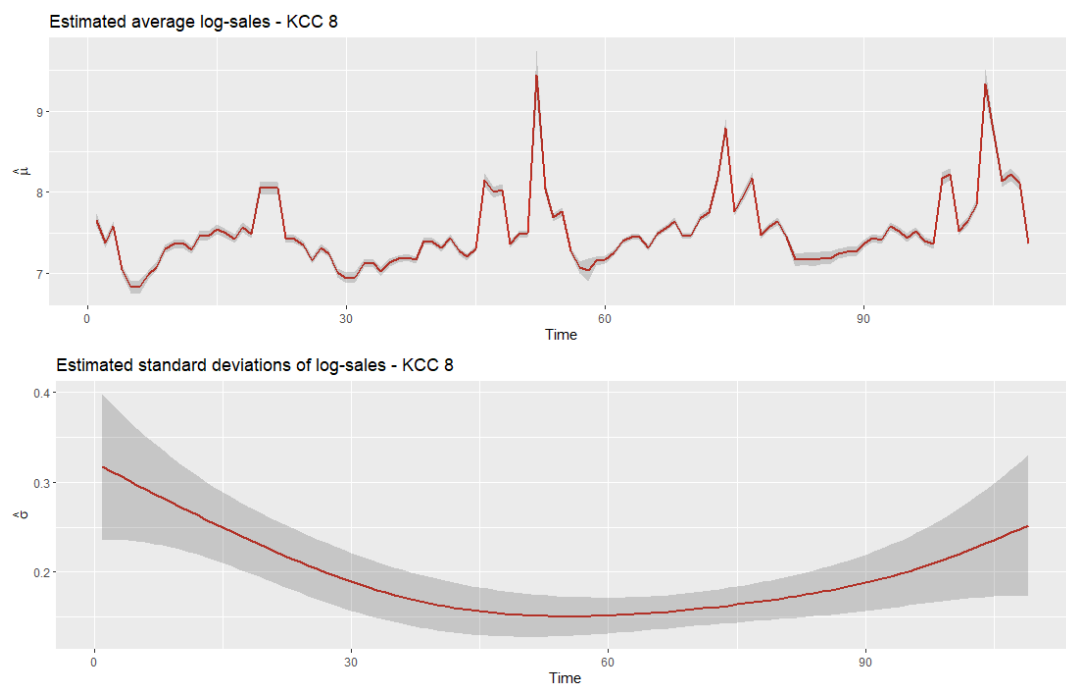


Figure 5.13: Estimated location parameter  $\hat{\mu}$  and scale parameter  $\hat{\sigma}$  with confidence bands of GAMLSS fit - KCC 8

Lower	$\hat{\nu}$	Upper
0.122	0.143	0.165

Table 5.6: Estimated skewness parameter  $\hat{\nu}$  of GAMLSS fit with 95% confidence interval bounds - KCC 8

The temporal effect exhibits the same shape as in KCC 6, collapsing into a straight line. Markdown effects are increasing as expected. Spring-Summer seems to have a slightly higher effect compared to Fall-Winter season in this cluster.

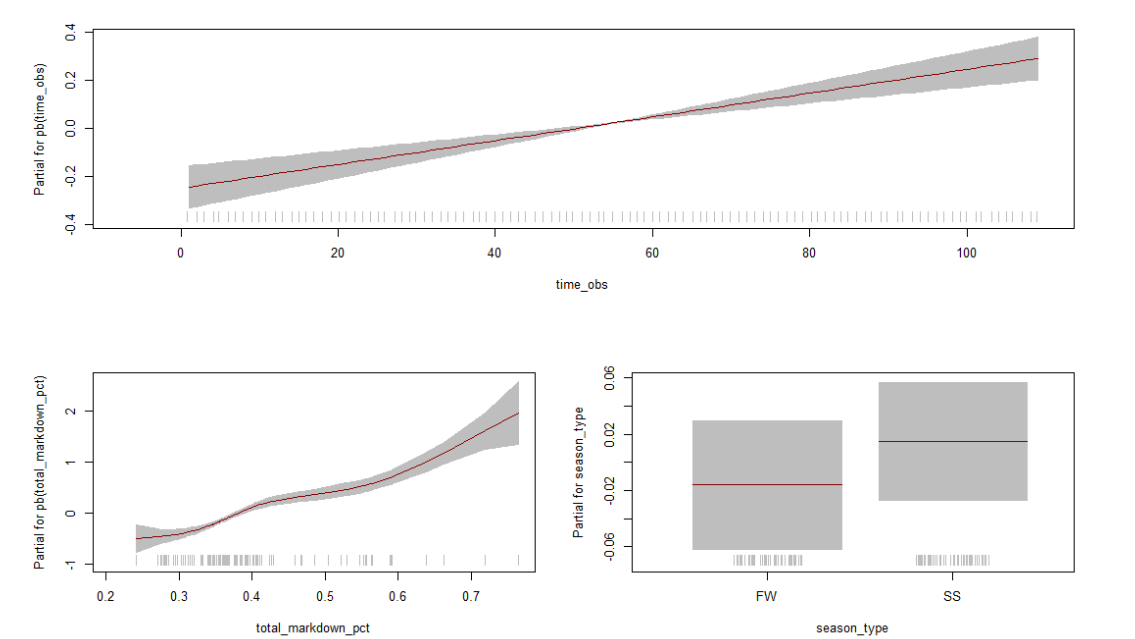


Figure 5.14: Covariate effects on the expected response variable (log-sales) of GAMLSS fit - KCC 8

Looking at Figure 5.15 and the summary output for the distribution of the quantile residuals, the fitting method for this cluster is also justified.

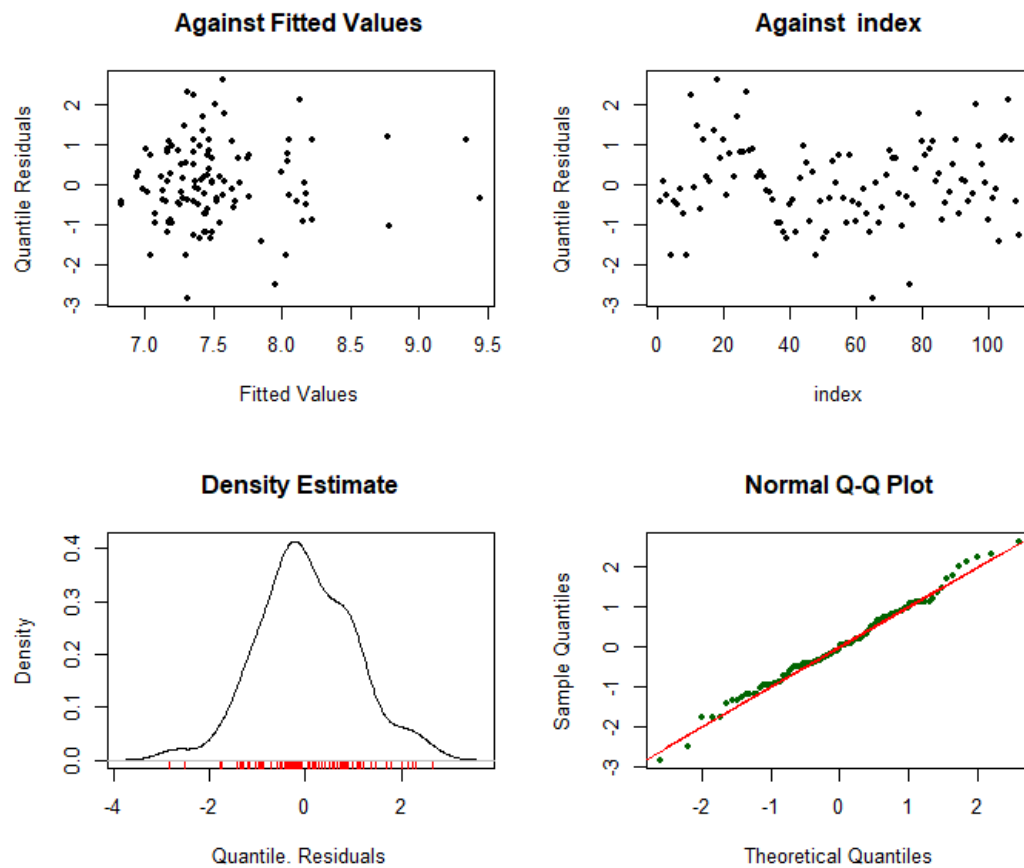


Figure 5.15: Residuals of GAMLSS fit - KCC 8

"Residuals of GAMLSS Fit on KCC 8"

```
*****
Summary of the Quantile Residuals
      mean    = 0.02392926
      variance = 1.005977
      coef. of skewness = 0.06145735
      coef. of kurtosis = 3.198929
Filliben correlation coefficient = 0.9953053
*****
```

## 5.2 KCC Correlations

## 5.3 Article Correlations

In this subsection we attempt to discover a dependence structure on the individual article unit sales. To do so, we will first delimit our data on article level (Subsection 5.3.1) to achieve lower dimensionality.

MAYBE WRITE STH ON USAGE OF VINES HERE..

### 5.3.1 Data Delimitation

On the lowest product hierarchy level, the number of unique articles is quite large for models to handle. In Table 5.7, we can see that our key category clusters of interest, 2, 6 and 8, have 1587, 9746 and 2012 articles respectively. Although we only work on those KCCs, even advanced techniques like vine copulas are struggling to handle such dimensions.

Key Category Cluster	1	2	3	4	5	6	7	8	9
Unique Articles	14	1,587	4,151	278	1,713	9,746	374	2,012	6,328

Table 5.7: Articles per Key Category Cluster

We have to take into consideration different models for each group. On top, further data delimitation shall reduce the dimensionality even further. Referring back to Table 1.1, we know that our last week of observation is "2018-12-24". We will restrict ourselves to articles that were not taken off the assortment before that date because they will most probably not be put back for sale.<sup>14</sup> After setting these boundaries, we arrive at a considerably smaller magnitude shown in Table 5.8.

Key Category Cluster	2	6	8
Unique Articles	39	256	58

Table 5.8: Articles per Key Category Cluster after data delimitation

---

<sup>14</sup>We neglect the possibility of an item to return in the future.





## 6 Conclusion



## List of Abbreviations

**AIC** Akaike Information Criterion

**BS** Business Segment

**CDF** Cumulative Distribution Function

**d.o.f.** Degrees of Freedom

**GAM** Generalized Additive Model

**GAMLSS** Generalized Additive Models for Location, Scale & Shape

**GAMM** Generalized Additive Mixed Model

**GLM** Generalized Linear Model

**GLMM** Generalized Linear Mixed Model

**GJRM** Generalized Joint Regression Models

**KC** Key Category

**KCC** Key Category Cluster

**LM** Linear Regression Model

**LMM** Linear Mixed Model

**PDF** Probability Density Function

**RV** Random Variable

**STAR** Structured Additive Regression Model



## List of Figures

1.1	Two of the adidas-group logos: Performance (left) & Originals (right) [adidas.com media-center]	2
1.2	adidas celebrates its 70th anniversary and the opening of the ARENA building [adidas 70 years, 2019]	2
3.1	Bivariate Gaussian distribution and Gaussian copula for Pearson's $\rho = 0.6$ and simulated sample of size $n = 1800$ , both with standard normal marginals	16
3.2	Bivariate t-distribution and t-copula with 3 degrees of freedom for Pearson's $\rho = 0.6$ and simulated sample of size $n = 1800$ , both with standard normal marginals	17
3.3	Shape of a generator function	18
3.4	Bivariate Clayton distribution and Clayton copula for Kendall's $\tau = 0.6$ and simulated sample of size $n = 1800$ , both with standard normal marginals	18
3.5	Bivariate Gumbel distribution and Gumbel copula for Kendall's $\tau = 0.6$ and simulated sample of size $n = 1800$ , both with standard normal marginals	19
3.6	Bivariate Frank distribution and Frank copula for Kendall's $\tau = 0.6$ and simulated sample of size $n = 1800$ , both with standard normal marginals	20
4.1	Illustration of a hierarchical article structure	25
4.2	Example of a single child node	26
4.3	Course of article unit sales	26
4.4	Scatterplots of promotion intensities against article unit sales; The y-axes are cut at 100	27
4.5	Unit sales in log-scale against total markdown percentage	28
4.6	Unit sales in log-scale against season type	28
4.7	Monthly patterns of article unit sales	29
4.8	Distribution of sold units of articles per week split at 200 units	30
4.9	Empirical CDF of all sold units per week; x-axis cut at 500	30
4.10	Time series and boxplot showing logarithmized sales of the key category clusters	31
4.11	Pairwise scatterplots of sales on KCC level. First row: Logarithmic sales with marginal densities, Second row: Pseudo sales observation with marginal histograms	32

4.12 Correlation plots of the three KCC log-sales with different correlation coefficients. Left: Pearson's rho, Middle: Kendall's tau, Right: Spearman's rho . . . . .	33
4.13 Boxplots showing log-sales of KCCs against presence of Black Friday . . . .	33
4.14 Boxplots showing log-sales of KCCs against presence of Friends & Family . .	34
4.15 Scatterplots of KCC log-sales against total markdown percentage . . . . .	34
4.16 Boxplots of KCC log-sales against the two season types . . . . .	34
5.1 exGaussian distribution fitted to log-sales of KCC 2 . . . . .	36
5.2 Residuals of KCC 2 log-sales fitted to an exGaussian distribution with no covariate effects together with their density curve . . . . .	36
5.3 Estimated location parameter $\hat{\mu}$ and scale parameter $\hat{\sigma}$ with confidence bands of GAMLSS fit - KCC 2 . . . . .	37
5.4 Covariate effects on the expected response variable (log-sales) of GAMLSS fit - KCC 2 . . . . .	40
5.5 Residuals of GAMLSS fit - KCC 2 . . . . .	41
5.6 exGaussian distribution fitted to log-sales of KCC 6 . . . . .	42
5.7 Residuals of KCC 6 log-sales fitted to an exGaussian distribution with no covariate effects together with their density curve . . . . .	42
5.8 Estimated location parameter $\hat{\mu}$ and scale parameter $\hat{\sigma}$ with confidence bands of GAMLSS fit - KCC 6 . . . . .	45
5.9 Covariate effects on the expected response variable (log-sales) of GAMLSS fit - KCC 6 . . . . .	46
5.10 Residuals of GAMLSS fit - KCC 6 . . . . .	47
5.11 exGaussian distribution fitted to log-sales of KCC 8 . . . . .	48
5.12 Residuals of KCC 8 log-sales fitted to an exGaussian distribution with no covariate effects together with their density curve . . . . .	48
5.13 Estimated location parameter $\hat{\mu}$ and scale parameter $\hat{\sigma}$ with confidence bands of GAMLSS fit - KCC 8 . . . . .	50
5.14 Covariate effects on the expected response variable (log-sales) of GAMLSS fit - KCC 8 . . . . .	51
5.15 Residuals of GAMLSS fit - KCC 8 . . . . .	52

## List of Tables

1.1	Transactional raw data description from online purchases of western European countries . . . . .	3
1.2	Article attribute data . . . . .	4
3.1	Bivariate relationships in copula families, with $T_\nu$ being the Student's t-distribution function with $\nu$ degrees of freedom and $D_k(x) = \frac{k}{x^k} \int_0^x \frac{t^k}{e^t - 1} dt$ being the Debye function [stanfordphd] . . . . .	23
4.1	Black Friday weeks . . . . .	27
4.2	Friends & Family weeks . . . . .	27
4.3	Number of sold units per week & number of affected articles for various quantiles of sales . . . . .	29
5.1	Estimated parameters for log-sales of KCC 2 fitted to exGaussian distribution with no covariate effects . . . . .	36
5.2	Estimated skewness parameter $\hat{\nu}$ of GAMLSS fit with 95% confidence interval bounds - KCC 2 . . . . .	38
5.3	Estimated parameters for log-sales of KCC 6 fitted to exGaussian distribution with no covariate effects . . . . .	42
5.4	Estimated skewness parameter $\hat{\nu}$ of GAMLSS fit with 95% confidence interval bounds - KCC 6 . . . . .	45
5.5	Estimated parameters for log-sales of KCC 8 fitted to exGaussian distribution with no covariate effects . . . . .	48
5.6	Estimated skewness parameter $\hat{\nu}$ of GAMLSS fit with 95% confidence interval bounds - KCC 8 . . . . .	51
5.7	Articles per Key Category Cluster . . . . .	53
5.8	Articles per Key Category Cluster after data delimitation . . . . .	53





## References

- [adidas 70 years 2019] adidas 70 years: *adidas celebrates its 70th anniversary and the opening of the ARENA building*. 2019. – <https://www.adidas-group.com/en/media/news-archive/press-releases/2019/adidas-celebrates-70th-anniversary>, Last accessed on 2020-04-01
- [adidas-group.com] adidas-group.com: *adidas-group*. – <https://www.adidas-group.com/en/>, Last accessed on 2020-04-01
- [adidas.com media-center] adidas.com media-center: *adidas media-center. Pictures and Videos*. – <https://www.adidas-group.com/en/media/media-center/>, Last accessed on 2020-04-01
- [Dagum 1975] Dagum, Camilo: A model of income distribution and the conditions of existence of moments of finite order. In: *Bulletin of the International Statistical Institute* 46 (1975), S. 199–205
- [Embrechts et al. 2001] Embrechts, Paul ; Lindskog, Filip ; McNeil, Alexander: Modelling dependence with copulas. In: *Rapport technique, Département de mathématiques, Institut Fédéral de Technologie de Zurich, Zurich* 14 (2001)
- [Fahrmeir et al. 2003] Fahrmeir, L. ; Kneib, T. ; Lang, S. ; Marx, B.: *Regression; Models, Methods and Applications*. 2013. 2003
- [Grushka 1972] Grushka, Eli: Characterization of exponentially modified Gaussian peaks in chromatography. In: *Analytical Chemistry* 44 (1972), Nr. 11, S. 1733–1738
- [Hastie and Tibshirani 1986] Hastie, Trevor ; Tibshirani, Robert: Generalized Additive Models. In: *Statist. Sci.* 1 (1986), 08, Nr. 3, S. 297–310. – URL <https://doi.org/10.1214/ss/1177013604>
- [Hastie and Tibshirani 1990] Hastie, Trevor J. ; Tibshirani, Robert J.: Generalized additive models, volume 43 of. In: *Monographs on statistics and applied probability* 15 (1990)
- [Hofert et al. 2019] Hofert, Marius ; Kojadinovic, Ivan ; Mächler, Martin ; Yan, Jun: *Elements of copula modeling with R*. Springer, 2019

- [Klein and Kneib 2016] Klein, Nadja ; Kneib, Thomas: Simultaneous inference in structured additive conditional copula regression models: a unifying Bayesian approach. In: *Statistics and Computing* 26 (2016), Nr. 4, S. 841–860
- [Marra and Radice 2016] Marra, G. ; Radice, R.: A Bivariate Copula Additive Model for Location, Scale and Shape. Cornell University Library (2017). In: *arXiv preprint arxiv:1605.07521* (2016)
- [Marra and Radice 2020] Marra, Giampiero ; Radice, Rosalba: GJRM-package: Generalised Joint Regression Modelling. (2020)
- [McNeil et al. 2015] McNeil, Alexander J. ; Frey, Rüdiger ; Embrechts, Paul: *Quantitative risk management: concepts, techniques and tools-revised edition*. Chap. Copulas and Dependence, Princeton university press, 2015
- [Patton 2006] Patton, Andrew J.: Modelling asymmetric exchange rate dependence. In: *International economic review* 47 (2006), Nr. 2, S. 527–556
- [R Core Team 2018] R Core Team: *R: A Language and Environment for Statistical Computing*. Vienna, Austria: R Foundation for Statistical Computing (Veranst.), 2018. – URL <https://www.R-project.org/>
- [Rigby and Stasinopoulos 2001] Rigby, R. A. ; Stasinopoulos, D. M.: The GAMLSS project: a flexible approach to statistical modelling. In: *New trends in statistical modelling: Proceedings of the 16th international workshop on statistical modelling* Bd. 337 University of Southern Denmark (Veranst.), 2001, S. 345
- [Rigby and Stasinopoulos 2005] Rigby, Robert A. ; Stasinopoulos, D. M.: Generalized additive models for location, scale and shape. In: *Journal of the Royal Statistical Society: Series C (Applied Statistics)* 54 (2005), Nr. 3, S. 507–554
- [Ruppert and Matteson 2015] Ruppert, David ; Matteson, David S.: *Copulas*. S. 183–215. In: *Statistics and Data Analysis for Financial Engineering: with R examples*. New York, NY : Springer New York, 2015. – URL [https://doi.org/10.1007/978-1-4939-2614-5\\_8](https://doi.org/10.1007/978-1-4939-2614-5_8). – ISBN 978-1-4939-2614-5
- [Schmidt 2007] Schmidt, Thorsten: Coping with copulas. In: *Copulas-From theory to application in finance* (2007), S. 3–34
- [Shapiro and Wilk 1965] Shapiro, Samuel S. ; Wilk, Martin B.: An analysis of variance test for normality (complete samples). In: *Biometrika* 52 (1965), Nr. 3/4, S. 591–611

- [Sklar 1959] Sklar, M.: Fonctions de repartition an dimensions et leurs marges. In: *Publ. inst. statist. univ. Paris* 8 (1959), S. 229–231
- [stanfordphd ] stanfordphd: *Copula*. – <https://stanfordphd.com/Copula.html>, Last accessed on 2020-04-27
- [Stasinopoulos et al. 2007] Stasinopoulos, D. M. ; Rigby, Robert A. et al.: Generalized additive models for location scale and shape (GAMLSS) in R. In: *Journal of Statistical Software* 23 (2007), Nr. 7, S. 1–46
- [Trivedi and Zimmer 2017] Trivedi, Pravin ; Zimmer, David: A note on identification of bivariate copulas for discrete count data. In: *Econometrics* 5 (2017), Nr. 1, S. 10
- [Vatter and Chavez-Demoulin 2015] Vatter, Thibault ; Chavez-Demoulin, Valérie: Generalized additive models for conditional dependence structures. In: *Journal of Multivariate Analysis* 141 (2015), S. 147–167
- [Vatter and Nagler 2018] Vatter, Thibault ; Nagler, Thomas: Generalized additive models for pair-copula constructions. In: *Journal of Computational and Graphical Statistics* 27 (2018), Nr. 4, S. 715–727
- [Vatter and Nagler 2019] Vatter, Thibault ; Nagler, Thomas: gamCopula-package: Generalized Additive Models for Bivariate Conditional... (2019)
- [Wood 2017] Wood, Simon N.: *Generalized additive models: an introduction with R*. CRC press, 2017